Edited by
VLADIMIR ANIKEEV
MAOHONG FAN

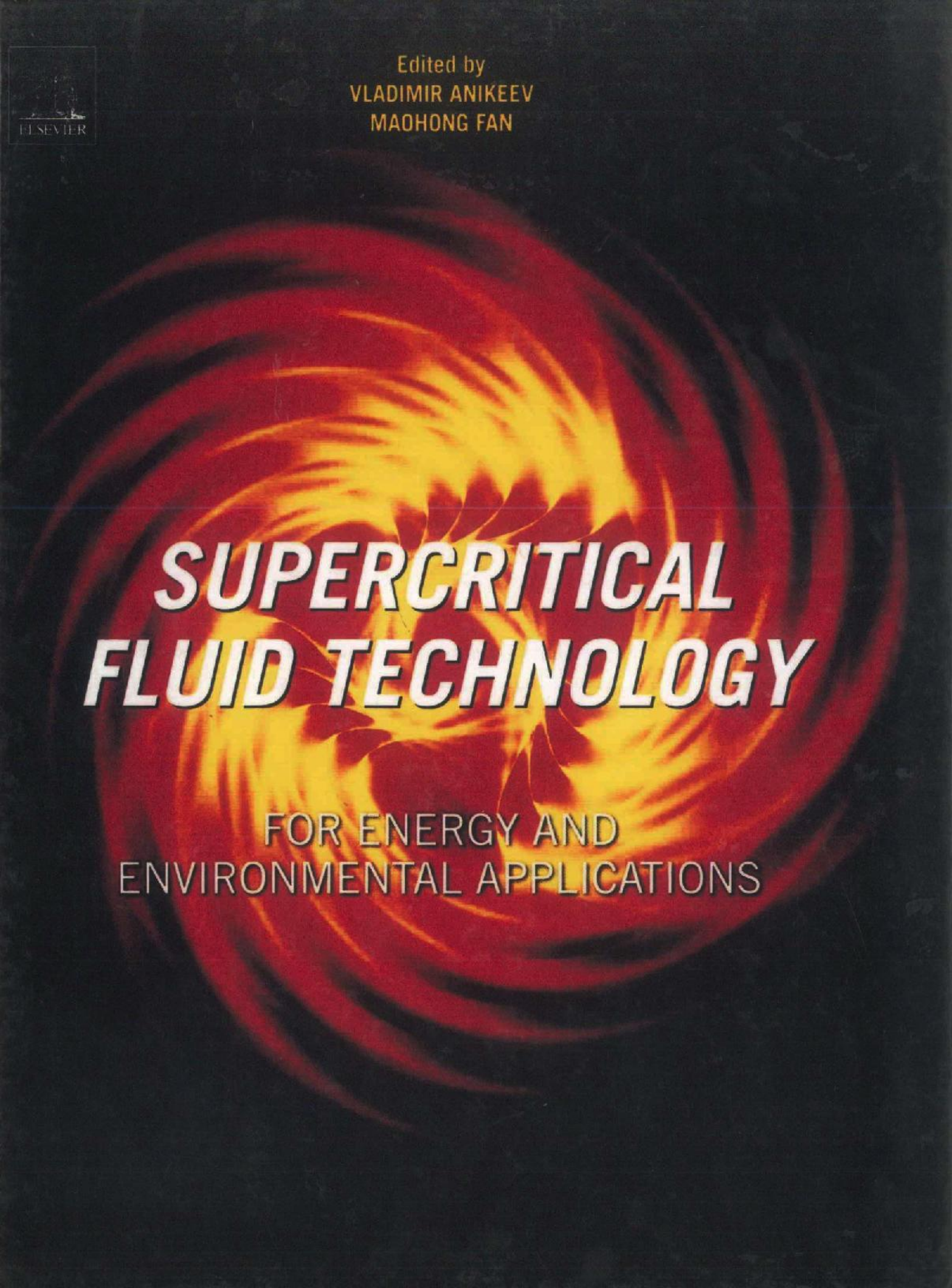

SUPERCRITICAL FLUID TECHNOLOGY

FOR ENERGY AND ENVIRONMENTAL APPLICATIONS

SUPERCRITICAL FLUID TECHNOLOGY FOR ENERGY AND ENVIRONMENTAL APPLICATIONS

Edited by

VLADIMIR ANIKEEV
Boreskov Institute of Catalysis, Novosibirsk, Russia

and

MAOHONG FAN
University of Wyoming
Laramie, WY, USA

ELSEVIER

AMSTERDAM • BOSTON • HEIDELBERG • LONDON
NEW YORK • OXFORD • PARIS • SAN DIEGO
SAN FRANCISCO • SYDNEY • TOKYO

Elsevier
Radarweg 29, PO Box 211, 1000 AE Amsterdam, The Netherlands
The Boulevard, Langford Lane, Kidlington, Oxford, OX5 1GB, UK
225 Wyman Street, Waltham, MA 02451, USA

British Library Cataloguing in Publication Data
A catalogue record for this book is available from the British Library

Library of Congress Cataloging-in-Publication Data
A catalog record for this book is available from the Library of Congress

ISBN: 978-0-444-62696-7

For information on all Elsevier publications visit our web site at store.elsevier.com

Printed and bound in Poland
14 15 16 17 18 10 9 8 7 6 5 4 3 2 1

Contents

Contributors vii

1. Synthesis of Biodiesel Fuel in Supercritical Lower Alcohols with and without Heterogeneous Catalysts (Thermodynamics, Phase and Chemical Equilibriums, Experimental Studies) 1
VLADIMIR I. ANIKEEV

2. Particle Formation Using Sub- and Supercritical Fluids 31
Ž. KNEZ, M. ŠKERGET, M. KNEZ HRNČIČ, D. ČUČEK

3. Environmentally Benign Transformations of Monoterpenes and Monoterpenoids in Supercritical Fluids 69
KONSTANTIN P. VOLCHO, VLADIMIR I. ANIKEEV

4. Biomass Conversion in Supercritical Water 89
TADAFUMI ADSCHIRI

5. Environmentally Benign Route for Nanomaterial Synthesis by Using SCW 99
NOBUAKI AOKI, DAISUKE HOJO, SEIICHI TAKAMI, TADAFUMI ADSCHIRI

6. Supercritical Water Gasification for Hydrogen Production: Current Status and Prospective of High-Temperature Operation 111
RATNA FRIDA SUSANTI, JAEHOON KIM, KI-PUNG YOO

7. Hydrolysis in Near- and Supercritical Water for Biomass Conversion and Material Recycling 139
ANNE LOPPINET-SERANI, CYRIL AYMONIER

8. Applications of Aerogels and Their Composites in Energy-Related Technologies 157
ZEYNEP ÜLKER, DENIZ SANLI, CAN ERKEY

9. Supercritical Water Oxidation for Wastewater Destruction with Energy Recovery 181
VIOLETA VADILLO, JEZABEL SÁNCHEZ-ONETO, JUAN R. PORTELA, ENRIQUE J. MARTÍNEZ DE LA OSSA

10. Supercritical Water Gasification of Organic Wastes for Energy Generation 191
M. BELÉN GARCÍA-JARANA, JEZABEL SÁNCHEZ ONETO, JUAN R. PORTELA, ENRIQUE J. MARTÍNEZ DE LA OSSA

11. Application of Supercritical Pressure in Power Engineering: Specifics of Thermophysical Properties and Forced-Convective Heat Transfer 201
IGOR PIORO

12. Biopolymer Degradation in Sub- and Supercritical Water for Biomass Waste Recycling 235
ARMANDO T. QUITAIN, MITSURU SASAKI, MOTONOBU GOTO

13. Energy Conversion of Biomass and Recycling of Waste Plastics Using Supercritical Fluid, Subcritical Fluid and High-Pressure Superheated Steam 249
IDZUMI OKAJIMA, TAKESHI SAKO

Index 269

Contributors

Tadafumi Adschiri World Premier International Research Center-Advanced Institute for Materials Research (WPI-AIMR), Tohoku University, Aoba, Sendai, Miyagi, Japan

Vladimir I. Anikeev Boreskov Institute of Catalysis, Siberian Branch of the Russian Academy of Sciences, Novosibirsk, Russian Federation

Nobuaki Aoki World Premier International Research Center-Advanced Institute for Materials Research (WPI-AIMR), Tohoku University, Aoba, Sendai, Miyagi, Japan

Cyril Aymonier CNRS, ICMCB, UPR9048, F-33600 Pessac, France; Univ. Bordeaux, ICMCB, UPR9048, F-33600 Pessac, France

D. Čuček Faculty of Chemistry and Chemical Engineering, University of Maribor, Slovenia

Can Erkey Department of Chemical and Biological Engineering, Koç University, Istanbul, Turkey

M. Belén García-Jarana Department of Chemical Engineering and Food Technology, Faculty of Sciences, Agro-Food International Excellence Campus CeiA3, University of Cádiz, Puerto Real, Cádiz, Spain

Motonobu Goto Department of Chemical Engineering, Nagoya University, Chikusa-ku, Nagoya, Japan

Daisuke Hojo World Premier International Research Center-Advanced Institute for Materials Research (WPI-AIMR), Tohoku University, Aoba, Sendai, Miyagi, Japan

M. Knez Hrnčič Faculty of Chemistry and Chemical Engineering, University of Maribor, Slovenia

Jaehoon Kim School of Mechanical Engineering, Sungkyunkwan University, Seobu-Ro, Jangan-Gu, Suwon, Gyeong Gi-Do, Republic of Korea; Sungkyun Advanced Institute of Nano Technology (SAINT), Seobu-Ro, Jangan-Gu, Suwon, Gyeong Gi-Do, Republic of Korea

Ž. Knez Faculty of Chemistry and Chemical Engineering, University of Maribor, Slovenia

Anne Loppinet-Serani CNRS, ICMCB, UPR9048, F-33600 Pessac, France; Univ. Bordeaux, ICMCB, UPR9048, F-33600 Pessac, France

Enrique J. Martínez de la Ossa Department of Chemical Engineering and Food Technology, Faculty of Sciences, Agro-Food International Excellence Campus CeiA3, University of Cádiz, Puerto Real, Cádiz, Spain

Idzumi Okajima Energy System Section, Graduate School of Science and Technology, Shizuoka University, Shizuoka, Japan

Igor Pioro Faculty of Energy Systems and Nuclear Science, University of Ontario Institute of Technology, Oshawa, ON, Canada

Juan R. Portela Department of Chemical Engineering and Food Technology, Faculty of Sciences, Agro-Food International Excellence Campus CeiA3, University of Cádiz, Puerto Real, Ca'diz, Spain

Armando T. Quitain Graduate School of Science and Technology, Kumamoto University, Chuo-ku, Kumamoto, Japan

Takeshi Sako Energy System Section, Graduate School of Science and Technology, Shizuoka University, Shizuoka, Japan

Jezabel Sánchez-Oneto Department of Chemical Engineering and Food Technology, Faculty of Sciences, Agro-Food International Excellence Campus CeiA3, University of Cádiz, Puerto Real, Cádiz, Spain

Deniz Sanli Department of Chemical and Biological Engineering, Koç University, Istanbul, Turkey

Mitsuru Sasaki Graduate School of Science and Technology, Kumamoto University, Chuo-ku, Kumamoto, Japan

M. Škerget Faculty of Chemistry and Chemical Engineering, University of Maribor, Slovenia

Ratna Frida Susanti Supercritical Fluid Research Laboratory, Clean Energy Research Center, Korea Institute of Science and Technology (KIST), Seongbuk-gu, Seoul, Republic of Korea; Chemical Engineering Department, Parahyangan Catholic University, Bandung, West Java, Indonesia

Seiichi Takami Institute of Multidisciplinary Research for Advanced Materials, Tohoku University, Aoba, Sendai, Miyagi, Japan

Zeynep Ülker Department of Chemical and Biological Engineering, Koç University, Istanbul, Turkey

Violeta Vadillo Department of Chemical Engineering and Food Technology, Faculty of Sciences, Agro-Food International Excellence Campus CeiA3, University of Cádiz, Puerto Real, Cádiz, Spain

Konstantin P. Volcho Vorozhtsov Novosibirsk Institute of Organic Chemistry, Siberian Branch of the Russian Academy of Sciences, Novosibirsk, Russian Federation

Ki-pung Yoo Department of Chemical and Biomolecular Engineering, Sogang University, Mapo-gu, Seoul, Republic of Korea

CHAPTER

6

Supercritical Water Gasification for Hydrogen Production: Current Status and Prospective of High-Temperature Operation

Ratna Frida Susanti [1,2], *Jaehoon Kim* [3,4], *Ki-pung Yoo* [5]

[1]Supercritical Fluid Research Laboratory, Clean Energy Research Center, Korea Institute of Science and Technology (KIST), Seongbuk-gu, Seoul, Republic of Korea, [2]Chemical Engineering Department, Parahyangan Catholic University, Bandung, West Java, Indonesia, [3]School of Mechanical Engineering, Sungkyunkwan University, Seobu-Ro, Jangan-Gu, Suwon, Gyeong Gi-Do, Republic of Korea, [4]Sungkyun Advanced Institute of Nano Technology (SAINT), Seobu-Ro, Jangan-Gu, Suwon, Gyeong Gi-Do, Republic of Korea, [5]Department of Chemical and Biomolecular Engineering, Sogang University, Mapo-gu, Seoul, Republic of Korea

OUTLINE

6.1 Introduction 112
- *6.1.1 Why Consider Hydrogen as a Future Energy Source?* 112
- *6.1.2 Hydrogen Sources and Production Technologies* 112
- *6.1.3 Strategies and Economic Considerations* 113

6.2 High-Temperature Water 113
- *6.2.1 Properties of Water* 113
- *6.2.2 Advantages of SCWG* 116
- *6.2.3 Disadvantages of SCWG* 117
- *6.2.4 Types of SCWG* 117
  - 6.2.4.1 Low-Temperature SCWG (~500 °C, Near-Critical Water) 117
  - 6.2.4.2 High-temperature SCWG (>500 °C) 118
- *6.2.5 Current Review Focus* 119

6.3 Thermodynamics of SCWG 119
- *6.3.1 Chemical Reactions* 119
- *6.3.2 Estimation of Theoretical Maximum Hydrogen Gas Yield* 121
- *6.3.3 Optimization of Operation Parameters* 121
  - 6.3.3.1 Temperature 121
  - 6.3.3.2 Pressure 122
  - 6.3.3.3 Feedstock Concentration 122
  - 6.3.3.4 Residence Time 123

6.4 Gasification of Simple Feedstocks 123
- *6.4.1 Methanol* 123
- *6.4.2 Ethanol* 124
- *6.4.3 Glucose* 126
- *6.4.4 Glycerol* 130
- *6.4.5 Model Compound for Lignin* 131

6.5 Gasification of Fossil Fuels 132

6.6 Challenges/Outlook 134

6.7 Conclusion 135

References 135

Supercritical Fluid Technology for Energy and Environmental Applications
http://dx.doi.org/10.1016/B978-0-444-62696-7.00006-X

Supercritical Fluid Technology for Energy and Environmental Applications, First Edition, 2014, 111–137

6.1 INTRODUCTION

6.1.1 Why Consider Hydrogen as a Future Energy Source?

Hydrogen is the lightest element with an atomic weight of 1.00797 and atomic number of 1. Moreover, hydrogen is the most abundant element in the universe (up to 75% by mass of all baryonic matter). However, hydrogen is not found in its free molecular form in a significant quantity. Most of the hydrogen is present in the compound form in water, hydrocarbons, and biomass. Therefore, biological, thermochemical, or electrochemical processes are required to free hydrogen from its compounds. Hydrogen has a wide variety of applications in chemical syntheses, food industries, refineries, and transportation. Among the applications, 40% is used for chemical processes, 40% for refineries, and 20% for others, including as energy carriers [1]. For example, hydrogen is utilized for the synthesis of ammonia and methanol, treatment of heavy crude oil, production of reformulated gasoline, desulfurization of middle distillate diesel fuel, catalytic hydrogenation of edible oils, hydrogenation of the nonedible oil used in soap manufacturing or animal feeds, and last, for fuel cell applications [2,3].

Furthermore, hydrogen has been demonstrated to be a potential clean energy carrier that can minimize our dependence on fossil fuels and reduce environmental pollution. Currently, most of the energy used in our daily lives comes from fossil fuels such as petroleum, coal, and natural gas, and they are the primary energy sources for transport, industry, electricity, and heat production. Our intensive dependence on fossil fuels causes serious environmental problems due to the emissions of green house gases and air pollutants (CO_2, NO_x, SO_x, etc.). In addition, the depletion of nonrenewable fossil fuel resources can cause serious geopolitical energy security problems. Hydrogen is a clean energy fuel because the chemical energy stored in the H−H bond is utilized when it is oxidized in an energy conversion system, e.g. fuel cells, which yields water as a by-product. Furthermore, hydrogen is a ubiquitous energy carrier because it can be produced from most of the feedstocks available everywhere in the world. Among chemical substances, hydrogen has the highest specific energy of 120 MJ/kg. Hydrogen and its utilization in fuel cells have been regarded as a potential clean energy alternative to support sustainable energy demands. Hydrogen is a secondary energy carrier that can be produced from various renewable primary energy sources such as water and biomass; further, it can be used in fuel cells for electricity generation and transportation. Fuel cells using hydrogen as an energy source lead to considerably higher thermodynamic efficiencies than conventional internal combustion engines, and moreover, air pollutants are not emitted. Therefore, the future of hydrogen as a clean energy source is closely related to the progress in fuel cell technologies.

6.1.2 Hydrogen Sources and Production Technologies

Both renewable (e.g. biomass and water) and nonrenewable energy sources (e.g. fossil fuels) are important for the development of hydrogen energy systems. Of course, for developing a truly sustainable energy system, hydrogen has to be produced from only renewable energy sources such as biomass, biofuels, and water, and the resulting energy system would be economically viable and self-sustaining. This is clearly a long-term ideal solution to fossil fuel depletions and environmental issues. During the transition period from carbon economy to hydrogen economy, hydrogen production from fossil fuels combined with carbon capture and storages to reduce carbon dioxide emissions would be an option for developing and supporting hydrogen energy systems.

The total global hydrogen production is presently around 60 Mt/year. Most of the hydrogen—approximately 96%—comes from fossil fuels (48% from steam reforming (SR) of natural gas, 30% from recovery of by-products of heavy hydrocarbon refinery, and 18% from coal gasification). Furthermore, water electrolysis, which is a dominant non-fossil-fuel-based hydrogen production method, currently accounts for 3.9% [4,5]. Various innovative hydrogen production methods that are based on renewable energy sources are the subject of ongoing research and development.

Hydrogen production technologies can be classified into three different types—thermochemical, electrochemical, and biological methods. Biological hydrogen production can be achieved via photosynthesis, fermentation, and microbial electrolysis cells. Although biological routes are environment friendly and less energy intensive than the other methods, biological hydrogen production is not ready to meet large-scale hydrogen production demands due to several limitations. Typically, the hydrogen production yield from the biological method is considerably lower than that from thermochemical or electrochemical hydrogen production method [2]. Thus far, the thermochemical (or reforming) method is the most mature technology [6]. Typically, the reforming method has considerably higher hydrogen production yields and more flexibility with feedstocks. At present, the SR of hydrocarbons, i.e. natural gas, is the most economical and most widely used process in industries to produce hydrogen [2,7,8]. The thermochemical conversion of biomass is considered as a

short-term technology for renewable hydrogen production. Biomass consists of all the living materials in the world, which may have different physical and chemical properties depending on their origin. Biomass-derived oxygenate compounds such as methanol, ethanol, and glycerol are also potential sources of hydrogen because they can be produced from renewable sources; moreover, hydrogen production from oxygenated compounds often requires mild reforming conditions [9]. Photochemical water splitting is a highly attractive hydrogen production alternative because the feedstock is renewable and carbon dioxide is not emitted.

6.1.3 Strategies and Economic Considerations

Due to its high energy density and environmental benignity, hydrogen is considered to be a promising future energy source. Nevertheless, there are many barriers to the commercialization of hydrogen as the main energy source, such as competition with other mature technologies, price distortions, and requirements of new infrastructure. There is still a long way to go before the stable state of hydrogen can be established as a clean and renewable energy form. In this situation, some strategies have been formulated to reduce the dependence of fossil fuels and simultaneously create nature-friendly technologies. In the short-term, some strategies would be based on today's combustion engines and infrastructures. The technologies developed are intended to utilize the current infrastructure for efficient hydrogen distributions as well as to use the available engines with marginal modifications.

Long-term strategies would focus on the development of electric engines driven by fuel cells, along with the establishment of mature renewable technologies and stabilization of the economy. Hydrogen fuel cells require huge investments for developing new engines, producing hydrogen on a large scale, and constructing hydrogen distribution infrastructure [10]. Nonetheless, hydrogen can be expected to be available at reasonable prices in the future, and hence, it may compete with gasoline or diesel fuel.

In 2007, the International Energy Agency (IEA) reported that the cost of decentralized (on site) hydrogen production exceeded $\$50/GJH_2$ [11]. For comparison, the price of oil was ~$10.5/GJ and the price of gasoline was ~$20/GJ. The Annual Merit Review in 2010 held by the Department of Energy in the United States reported that the hydrogen cost at stations in 2009 were $7.70−10.30/kg (from natural gas) and $10.00−12.90/kg (from electrolysis) [12]. According to the current data from the US Energy Information Administration, the cost of distributed US gasoline on 18 April 2011, was in the range of $3.609−4.205/gal (or $1.30−1.52/kg; assuming ρ gasoline = 0.73 kg/l), depending on the location, i.e. the state. In summary, hydrogen continues to be more expensive than gasoline or diesel fuel.

Liquefaction and transportation costs contribute significantly to the total hydrogen cost. The costs of the liquefaction and distribution of liquid hydrogen adds $7−10/GJ to the onsite hydrogen cost. Hydrogen liquefaction and distribution were more expensive than large-scale distributions by pipelines ($1−2/GJ of hydrogen cost). Refueling stations might add $3−9/GJ to the hydrogen cost [11]. Based on the data tabulated in the literature from 2002 to 2009 and the predicted costs of renewable hydrogen and fossil fuel from several prestigious agencies, Lemus et al. [13] evaluated that the predicted hydrogen cost from several alternative sources in the future (2019−2020 and 2030) is comparable to that from the conventional method (steam methane reforming (SMR) and coal gasification). For example, in centralized facilities (where liquefaction costs are added), among the other renewable hydrogen productions, only hydrogen produced from biomass gasification is currently at parity with coal gasification and SMR having an efficiency of 69%. The entire renewable hydrogen production will achieve cost parity in 2030 with coal gasification (with additional carbon tax of $50/GJ) and after 2021 with the SMR method (efficiency of 69%). On the other hand, in distributed facilities (without the addition of liquefaction costs), at present, none of the renewable hydrogen productions have parity with SMR. Further, the cost of fossil fuel resources in the future is the determinant factor of the cost parities. Hence, the strategies should focus on developing a more efficient reforming method to suppress hydrogen cost.

6.2 HIGH-TEMPERATURE WATER

6.2.1 Properties of Water

Water is an ecologically safe and environmentally benign substance that is present throughout nature. Under ambient conditions (25 °C, 1 atm), liquid water with a density of 997.05 kg/m^3 coexists with water vapor with a density of 0.0231 kg/m^3, and they are separated by a liquid−vapor phase boundary [14]. As the temperature and pressure increase, the water in the liquid state expands and becomes vapor. Consequently, the density of liquid water decreases, while the density of gas increases until the pressure and temperature reach a critical point ($T_c = 374$ °C, $P_c = 221$ bar, $\rho_c = 322$ kg/m^3) [15] wherein the liquid and gas densities are equal and the boundary layer between liquid and vapor is nonexistent. Supercritical water is water present at a state above its critical temperature and pressure. Table 6.1 lists the properties of water at different states while Figure 6.1 shows the physicochemical properties of

TABLE 6.1 Physicochemical Properties of Water in Different States

	Water	Superheated Steam	Subcritical Water	Supercritical Water		
T (°C)	25	400	300	400	400	700
P (MPa)	0.1	0.1	25	25	50	25
ρ (kg/m^3)	997.05	0.32	743.01	166.53	577.74	60.08
ε	78.4	1.005	21.48	3.81	12	1.29
pK_w	13.99	NA	11.12	16.57	11.56	19.83
μ (mPa s)	0.89	0.024	0.092	0.029	0.068	0.038

water at high temperatures and pressures. The densities of supercritical water are two or three orders of magnitude higher than those of steam, depending on the pressures and temperatures. Further, beyond the critical point, the density of supercritical water can be varied from liquidlike densities to gaslike densities by adjusting the temperature and pressure without changing the phase.

As shown in Figure 6.1, the ionic product of water (K_w) increases up to three orders of magnitude from its value under ambient conditions at temperatures between 200 and 300 °C. Accordingly, at subcritical and near-critical regions, water can act as an acid or base catalyst for various reactions; the ionic reaction mechanism is favored owing to the higher concentrations of [H_3O^+] and [OH^-] ions [16]. Examples of acid-catalyzed reactions of organic compounds in pure subcritical or near-critical water include the dehydration of 2-methylcyclohexanol to 1-methylcyclohexene [17], lactic acid to acrylic acid [18], cyclohexanol to cyclohexene [17], Friedel–Craft alkylation of phenol with *tert*-butyl alcohol to 2-tert-butylphenol and 4-tert-butylphenol [19], Beckmann rearrangement of cyclohexanone oxime to ε-caprolactam [20], and pinacol rearrangement to pinacolone [17,20]. Examples of base-catalyzed reactions in subcritical or near-critical water include the aldol condensation of *n*-butyraldehyde to 2-ethylhexanal, Dieckmann condensation of adipic acid and its dimethyl and diethyl esters to cyclopentanone [21], Claisen–Schmidt reaction of benzaldehyde to benzyl alcohol and benzoic acid [22], and Canizzaro-type reactions of formaldehyde to methanol and formic acid [23]. It is to be noted that high concentrations of [H_3O^+] and [OH^-] ions can also cause severe corrosion [24–26]. Typically, the corrosion is more severe in the subcritical region than in the

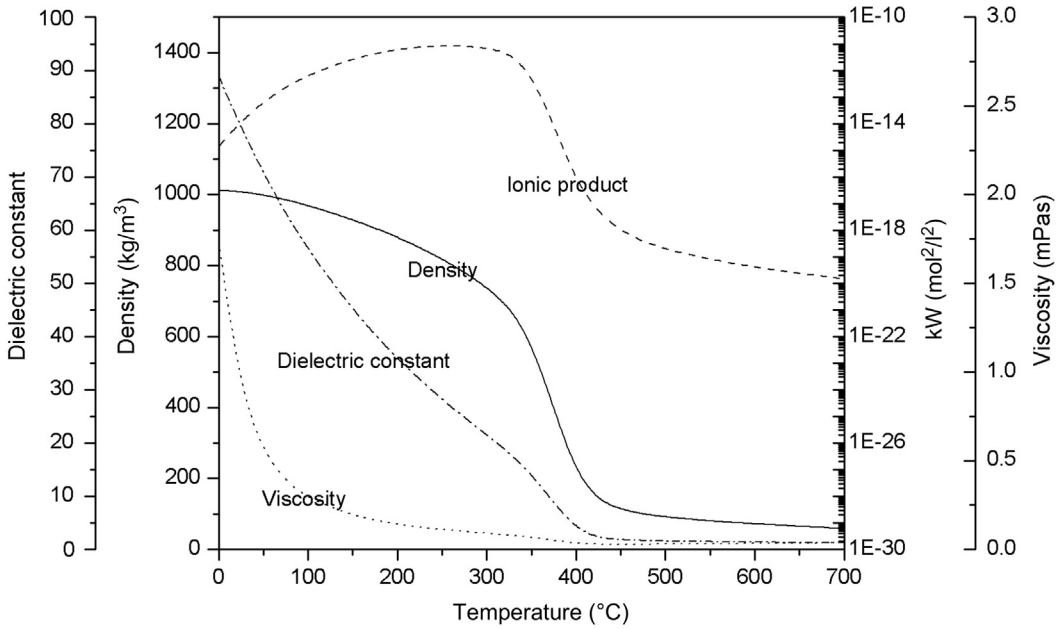

FIGURE 6.1 Selected properties of water as a function of temperature at 250 bar. *Data taken from Refs [14,155].*

supercritical region because water loses its ability to solvate charged species in the supercritical region.

In addition to the acid- and base-catalyzed reactions, the high concentrations of $[H_3O^+]$ and $[OH^-]$ ions make high-temperature water play the role of a reactant in hydrolysis reactions through the following mechanism:

$$A{-}B + H{-}OH \rightarrow A{-}H + B{-}OH$$

The hydrolysis reaction is typically catalyzed by acids or bases [27,28], and hence, the higher ion products in high-temperature water can have catalytic effects on the hydrolysis reaction. Heteroatom-containing hydrocarbon compounds such as ethers, esters, amines, amides, and nitroalkanes are particularly susceptible to the hydrolysis reaction [29,30].

As shown in Figure 6.1, the ionic product decreases dramatically above the critical point. For example, K_w is three orders of magnitude lower at 400 °C and 250 bar and six orders of magnitude lower at 700 °C and 250 bar than K_w of water under ambient conditions. At these high-temperature and low-density regimes, free radical reactions dominate the ionic reaction mechanism [24,31]. Examples of free radical reactions in high-temperature water include supercritical water oxidation (SCWO) and pyrolysis of biomass. For example, in the pyrolysis of glycerol, the formation of acetaldehyde and formaldehyde, which are supposed to be the products of ionic reactions, decreases, while that of allyl alcohol and methanol, which are supposed to be free radical reaction products, increases as the temperature increases from 357 °C to 477 °C as a result of the dominant free radical reaction at higher temperatures and lower densities [31]. In high-temperature ranges, SCWO is dominated by the free radical mechanism [32]. The reaction is initiated by the formation of a hydroxyl radical (•OH) that has strong electrophilic reactivity. The hydroxyl radical can react with almost all hydrogen-containing compounds producing (R•) and also react further with oxygen to form a peroxy radical; this can lead to hydrogen that can then be used for peroxide production. The peroxide decomposes further to organic compounds such as acetic acid and formic acid that can finally oxidize to CO_2 and H_2O. Gaseous products are typical products of free radical reactions.

$$H_2O_2 \rightarrow 2OH\bullet$$

$$RH + \bullet OH \rightarrow R\bullet + H_2O$$

$$R\bullet + O_2 \rightarrow ROO\bullet$$

$$ROO\bullet + RH \rightarrow ROOH + R\bullet$$

The viscosity of supercritical water is considerably lower than that of water under ambient conditions and slightly higher than that of steam (see Table 6.1). Figure 6.1 shows that the viscosity of water decreases significantly from 0.89 to 0.03 mPas as the temperature increases from 25 °C to 400 °C. The low viscosity reflects high molecular mobilities because the diffusion coefficient (D) is inversely proportional to viscosity or η, as given by the Stokes–Einstein relation [33,34]:

$$D = \frac{k_B T}{6\pi\eta r}$$

Accordingly, the high diffusion rate and low viscosity associated with supercritical water make it an efficient reaction medium especially for heterogeneously catalyzed reactions because mass transfer limitations can be avoided and the reaction rate can be increased.

The dielectric constant or static relative permittivity (ε) of water determines its solution properties such as the solubility of ionic and organic substances [35]. The dielectric constant of water decreases within creasing temperature and decreasing density [25]. For example, the dielectric constant of water at 300 °C and 743 kg/m^3 is 21.48, while that at 700 °C and 60 kg/m^3 is 1.29; note that these values are considerably lower than the value for ambient liquid water (78, see Table 6.1). As a result, by adjusting the temperature and pressure, water can be reached to a state where it can dissolve nonpolar organic compounds while simultaneously having good solubility of polar or ionic compounds. Gaseous substances are also completely miscible with supercritical water, while gases have very limited solubility in ambient liquid water. For example, the solubilities of methane, ethylene, ethane, carbon monoxide, carbon dioxide, and hydrogen in water at 20 °C and 0.1 MPa are ~0.023, ~0.15, ~0.06, ~0.028, ~1.7, and ~0.0016 g gas/kg of water, respectively [36]. By increasing the pressure and temperature, the solubilities of the above gases and other gases such as alkanes, benzene, xenon, and oxygen in water increase; finally, above the critical point of water, the gases become completely miscible with water [25]. The high solubility of nonpolar organic compounds, the complete miscibility with gases, and the low viscosity make supercritical water an excellent solvent that can run single-phase reactions and promote the reaction rate.

Several salts have positive solubility trends with increasing temperatures, and this has been investigated from the critical point of water to the critical point of the salt component [37]. The type of salt includes alkali and alkaline earth halides and hydroxides, which are categorized as type 1 salts; here, the three-phase solubility curve (L–G–S) does not intersect the critical curve (L–G). The salts categorized in the first type include NaOH, KOH, KCl, LiCl, NaCl, KBr, KI, H_2SO_4, $(NH4)_2SO_4$, H_3PO_4, K_2CO_3, $RbCO_3$, $Na_2B_4O_7$, and $CsNO_3$ [25,37]. However, if the water density decreases, this salt tends to precipitate. Other salts such as Na_2SO_4,

K_2SO_4, Li_2SO_4, Na_2CO_3, Li_2CO_3, LiF, NaF, CaF_2, BaF_2, and $CaSO_4$ are completely insoluble in supercritical water. They are classified as type 2 salts wherein the S−L−G three-phase line intersects the critical curve L−G. It is to be noted that most of the inorganic salts have limited solubility at pressure and temperature ranges that are attractive for many practical applications. Therefore, understanding the salt solubility behavior in supercritical water is extremely important to avoid reactor plugging due to salt precipitation and ineffective reactions due to lack of solubility. The strong dependence of inorganic salt solubility on temperature and density has been used to precipitate metal oxide particles with controlled sizes and shapes [38−42].

As the temperature increases and density decreases, the hydrogen bonding in water becomes weaker; further, the average number of water molecules that are connected by hydrogen bonding decreases [43−45]. Hoffmann and Conradi [46] summarized the persistence of hydrogen bonding based on their experiments using nuclear magnetic resonance and compared their results with those of other researchers using various methods such as molecular dynamics calculations, neutron diffraction based on isotopic substitution techniques, and Raman, infrared, and Monte Carlo simulation. At 400 °C ($\rho \sim 0.5\ g/cm^3$), the hydrogen bonding that persisted in water was 29−45%, while at 500 °C, ($\rho \sim 0.2$−$0.25\ g/cm^3$), the hydrogen bonding was 13−29% that of water under ambient conditions (25 °C). The weak and reduced number of hydrogen bondings in high-temperature water is known to be responsible for the low dielectric constant [25]. Furthermore, the breakdown of hydrogen bonding networks reduces the barriers against the rotational and translation motions of a water molecule. Accordingly, this enhances the mobility of single water molecules and increases self-diffusivity [47,48].

Various experimental data support the theory that water can provide hydrogen atoms to reactants in high-temperature water [49−52]. Park et al. [53] conducted gasification experiments of naphthalene in the presence of RuO_2 catalysts in supercritical deuterium oxide (D_2O) instead of supercritical H_2O. The gas chromatography/mass spectrometry (GC/MS) results showed that most of the produced gases were the entirely deuterated forms of CD_4 and D_2 and not CHD_3, H_2, or HD. This indicates that deuterium in supercritical D_2O is incorporated into the gaseous products. The ability of water to provide hydrogen plays a significant role in determining the product distribution in pyrolysis reactions and supercritical water gasification (SCWG). During the pyrolysis of organic substances such as polyethylene and polystyrene, hydrogen donation can promote the chain termination reaction in free radical chemistry, thereby enhancing the production of smaller molecular weight compounds and suppressing the formation of high-molecular-weight species, e.g. cross-linked products. Along with the high solvency of organic species, the hydrogen-releasing ability associated with high-temperature water can suppress char or tar formation during SCWG.

In addition to the supply of hydrogen atoms, high-temperature water can generate hydrogen molecules via the water-gas-shift reaction (WGS, $CO + H_2O \leftrightarrow H_2 + CO_2$, $\Delta H_{298K} = -41.15\ kJ/mol$) in the presence of carbon monoxide. This is an important reaction that can enhance hydrogen gas yields during typical SCWG. In supercritical water, the WGS mechanism can be promoted in the absence of catalysts [54], since excess amounts of water can drive the equilibrium of WGS reactions in the forward direction. The role of WGS reaction in reforming will be discussed in more detail in Section 6.3.1.

6.2.2 Advantages of SCWG

Water plays many different roles during the reforming under supercritical water conditions, and several advantages of using water are described below:

1. *High solubility of reaction intermediates*: This can reduce tar/coke formations; the reaction intermediates during their formation often have double bonds that can be polymerized into coke/tar. The high solubility of intermediates in supercritical water promotes collisions between water and single organic molecules more than collisions between organic molecules [55].
2. *High solubility of produced gas*: This can promote single-phase reactions. The typical gases present under SCWG condition include alkanes, carbon monoxide, hydrogen, carbon dioxide, and oxygen that are completely miscible with supercritical water [25].
3. *SCWG can deal with high water content of biomass*: This characteristic can eliminate high-energy-intensive drying steps such as vaporization during pyrolysis or distillation during biochemical processing [56,57]. Wet biomass such as water hyacinth and sewage sludges often has water content more than 80% [58]. Typical thermochemical biomass processes such as pyrolysis and conventional gasification require the water content to be below 10 wt% [55].
4. *Various feedstocks*: Due to the variations in the dielectric constant in supercritical water by controlling density and temperature, water can act as a polar, semipolar, or nonpolar solvent. The ability of supercritical water to solve hydrocarbon species, which are typical feedstocks for hydrogen production, can reduce the mass transfer barriers

inherent in multiphase reaction systems in conventional reforming processes.

5. *High working pressures lead to high densities of fluid phase*: High working pressures allow the development of compact gasification systems including reactors and subsequent units [59]. In addition, the single-phase reaction and low mass transfer resistance in supercritical water enable the gasification of feedstocks with a very short residence time reaction and utilization of small-size reactors [60]. The high pressures of the hydrogen produced can be stored directly, and this can eliminate the cost for pressurizing the produced gas.
6. *Fast hydrolysis and pyrolysis reactions*: Reduced mass transfer limitations and single-phase reactions can promote the gasification reaction.

6.2.3 Disadvantages of SCWG

Several disadvantages of the SCWG of liquid-type feedstocks are described below:

1. *High-temperature and high-pressure operations*: The high-temperature and high-pressure operations require specialized material for reactors and subsequent units and excellent operational safety. There are three considerations for material selection: corrosion, pressure resistance, and hydrogen aging [61]. The mechanical constraints caused by the high-pressure and high-temperature reactions and hydrogen contact, which possibly weaken the material strength, require the utilization of a suitable reactor material. Overall, high investment costs are required for developing the gasification system.
2. *Endothermic reforming reaction*: Since the reforming reaction is endothermic, high temperatures are favored for high hydrogen production yields. The high-temperature operations require severe external heating and large energy consumptions. To increase the energy efficiency of the entire gasification system, the reaction heat should be recovered by an efficient heat exchanger. This includes heat recovery from hot effluent stream and heat supply to incoming cold stream. Heat recovery will be a more important factor for designing a commercial-scale, cost-effective SCWG system.
3. *Low solubility of salt*: As discussed in Section 6.2.1, the limited solubility of salt in supercritical water can cause the clogging of reactors or associated pipings and the plugging of pores of heterogeneous catalysts if the reactions are not properly controlled. This problem will be more severe when feedstocks containing large amounts of inorganic impurities are used. However, it is to be noted that inorganic species in the feed can catalyze the WGS reactions, leading to high hydrogen gas yields [62,63]. In addition, the precipitated and separated inorganic species as a by-product can provide the opportunity to produce valuable chemicals such as fertilizers.

6.2.4 Types of SCWG

The operating conditions of SCWG determine the product gas composition. If hydrogen is the preferred product, temperatures of >600 °C are desirable at supercritical pressures. Milder temperatures (~500 °C) are often used to produce hydrogen with the catalyst addition. At lower temperatures (~400 °C), methane is the dominant product. Gasification in supercritical water can be categorized into two parts: low-temperature ($T < 500$ °C) and high-temperature gasification ($T > 500$ °C).

6.2.4.1 Low-Temperature SCWG (~500 °C, Near-Critical Water)

The objective of low-temperature SCWG is to produce methane-rich gas (near the supercritical region) or hydrogen (in the supercritical region) under mild conditions. The hydrogen gas yield from the low-temperature SCWG in the absence of catalysts is very low due to the endothermic nature of the reforming reaction. As shown in Figure 6.2, methane is the dominant product, while hydrogen is the minor product at temperatures below 420 °C. Methane is formed through the decarboxylation of acetic acid and decarbonylation of acetaldehyde or can be formed from the hydrogenation of carbon dioxide or carbon monoxide. As the

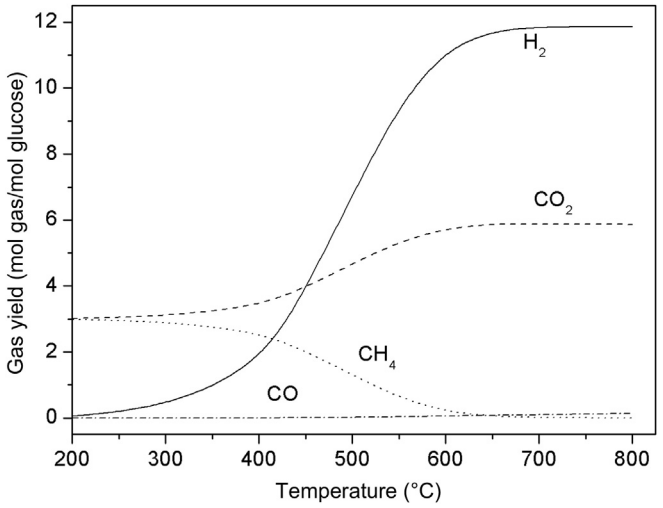

FIGURE 6.2 The gaseous yield at equilibrium in terms of composition ratio as a function of temperature for SCWG of 1.8 wt% glucose at 250 bar. The composition was calculated using Gibbs free energy minimization and Peng–Robinson equation of state.

temperature increases, the amount of hydrogen in the gas mixture increases.

The reactive intermediates formed during the biomass gasification, which are called water-soluble products (WSPs), will react further through two competing reaction pathways to produce gaseous products and oily products. Oil will then polymerize to form char, while the oily product, once it is formed, would not be gasified further. The role of catalysts in the low-temperature SCWG is to either inhibit the polymerization of oil or promote the conversion of the reactive intermediates to gaseous products [64–66]. Catalysts will increase the reaction rate to the desired gaseous product or increase the product selectivity. However, it is very difficult to achieve complete gasification in low-temperature SCWGs even in the presence of catalysts.

Either a homogenous or a heterogeneous catalyst can be used in SCWGs. Various types of heterogeneous catalysts have been tested in SCWG, such as activated carbon (AC) and supported metal catalysts such as nickel, rhodium, ruthenium, platinum, and palladium [16,67]. Studies on AC catalysts were conducted by Prof. Antal's groups over a high-temperature range [68–70]. Supported nickel catalysts can enhance methanation reaction, thereby leading to high methane gas yields. Elliot [67] tabulated the gasification of wet biomass at 400 °C, 15 min using a nickel-supported alumina-silica catalyst; 20–46% of the product was methane, while hydrogen comprised only 3–28% of the gas composition, depending on the kind of wet biomass feedstock. Nickel catalysts can be used if methane is the target product at low reaction temperatures below 400 °C [71]. In the case of noble metal catalysts, ruthenium and rhodium have higher catalyst activities than other noble metal catalysts such as platinum and palladium [72,73]. Significant amounts of methane were produced under near-critical conditions during the utilization of $Ru/\gamma - Al_2O_3$, $Ru/\delta - Al_2O_3$, Ru/ZrO_2, and Ru/carbon (reduced) catalysts [72]. The advantages of heterogeneous catalysts are easy separation and recovery, and moreover, they are also noncorrosive. However, a significant challenge of the supported catalysts is the catalyst lifetime. Most of the supported catalysts can give higher gas yields during short-term investigations, while they would be deactivated after several hours due to carbon/tarry compound formations on the catalysts [68,74,75], or due to the presence of sulfur- [76–79] or nitrogen-containing compounds [79] in the feeds. For instance, the carbon catalyst lost its activity after 4-h reactions, while its ability to accelerate the WGS reaction started to decrease after 2 h [68]. For the lignin gasification at 400 °C and 180 min reaction time, the presence of sulfur in the feed led to a decrease in the gas yield from 97.7 to 21.0 C% and an increase in the insoluble product (namely, char) yield from 0 to 3.1 C% [78]. Several studies have shown that certain types of supported catalysts have long-term stability in SCWG. The ruthenium on rutile-type TiO_2 was stable up to 3000-h operations under 350 °C, 210 bar during the gasification of wet organics [80]. The stabilized nickel catalyst with 1 wt% ruthenium loading developed by Elliot et al. [81] was found to be very active for at least 6 months during the gasification at 350 °C and ~340 bar. Another challenge during the utilization of heterogeneous catalysts in SCWG is plugging by the salts present in biomass feedstocks [55,82]. More severe plugging can happen in the presence of supported catalysts because the cross-sectional area of a reactor is narrower than in the case without catalysts.

Alkali compounds such as KOH, NaOH, LiOH, K_2CO_3, and Na_2CO_3 have been used as homogeneous catalysts in SCWGs [16,83]. The alkali catalysts increase the hydrogen gas yield by promoting the WGS reaction through formate formation [83,84]. The alkali addition also increases the reactor wall activity to catalyze the gasification reaction. Further, the oxide solubility is also increased, and hence, the detachment of the passivating layer on the reactor wall promotes the reactor surface activation to catalyze the gasification reaction [83]. The addition of alkali catalysts may lead to the formation of carbonates from their reaction with carbon dioxide, thereby decreasing the carbon dioxide amounts in gaseous products; they cause the equilibrium of the water–gas reaction to shift to the right for hydrogen formation [85]. Further, the tar/char formation is also decreased [86]. On the other hand, the use of alkali salt as a catalyst can cause plugging problems in the reactor or pipe due to its low solubility in supercritical water. Further, a solution with high pH, which is obtained by adding alkali salts, can corrode the reactor wall. The recovery of the remaining alkali catalysts is also important from the economic view point.

6.2.4.2 *High-temperature SCWG (>500 °C)*

Temperature plays a significant role in the gasification reaction and gas composition, especially in the absence of catalysts [60]. High-temperature conditions are required to achieve high reaction yields and selectivities. High temperatures promote the free radical reaction that is necessary for gas formation [31]. In contrast to low-temperature SCWGs, high-temperature SCWGs are favored for high hydrogen gas yields by the suppression of the methane formation. High reaction temperatures can be a potential alternative to avoid reactor plugging issues in biomass gasification [56,87]. High-temperature gasification is sometimes considered as inefficient because high external energy is needed. However, development of an efficient heat exchanger design will increase the energy efficiency of total gasification

systems. Further, the application of catalysts can lower the reaction temperature.

Since the past two decades, a large proportion of works on high-temperature SCWGs to produce hydrogen have been performed by five major research groups: Prof. Antal and coworkers at the University of Hawaii (USA), Prof. Swaaij and coworkers at the University of Twente (Netherlands), Prof. Matsumura and coworkers at the Hiroshima University (Japan), Prof. Guo and coworkers at the Xi'an Jiaotong University (China), and Drs. Kruse/Dinjus/Boukis and coworkers at Forschungszentrum Karlsruhe (Germany). Due to the recent interest in the role of supercritical water in the production of renewable fuels and chemicals, new research groups have made significant contributions. This includes Prof. Lee's group at Missouri University of Science and Technology, USA; Prof. Gupta's group at the Auburn University, USA; Prof. Savage's group at the University of Michigan, USA; and Prof. Williams and Dr Onwudili at the University of Leeds, UK.

6.2.5 Current Review Focus

There are several excellent reviews on gasification in supercritical water. Most reviews on the gasification of biomass in supercritical water had different focuses such as the status and prospects of biomass gasification in near-critical and supercritical water [88], the present state of the art of biomass gasification in supercritical water and major observations of small-scale laboratory flow and batch reactors [89], hydrothermal biomass gasification focusing on the utilization of heterogeneous catalysts [67] and nonutilization of heterogeneous catalysts [55] (as well as both simultaneously [16]), and the experiences gained from advanced continuous plants and challenges to overcome the SCWG of biomass [90]. Other reviews related to biofuel production in subcritical and supercritical water focus on the chemistry and engineering sciences associated with the hydrothermal processing of a range of biomass feedstock including liquefaction and gasification [57] and on the corrosion control method in the case of both SCWO and gasification [26]. In this review, we focus on the SCWG of simple liquid feedstocks and model compounds of biomass. To gain better understanding into the thermodynamic and hydrogen production mechanism in supercritical water, the hydrogen gas yield of each feedstock reformed under different conditions are compared with the theoretical equilibrium yield calculated by the Gibbs free energy minimization. The feedstocks that are reviewed in this work include methanol, ethanol, glucose, glycerol, model compounds of lignin, and liquid-type fossil fuels. Section 6.3 begins with thermodynamic considerations of the supercritical gasification reaction and includes chemical reactions, theoretical hydrogen yield calculations, and optimizations of the operation variable. Section 6.4 focuses on the gasification of simple feedstocks and model biomass compounds, while Section 6.5 discusses the gasification of liquid-type fossil fuel feedstocks. Finally, section 6.6 discusses the challenges, research requirements, and prospects for practical applications of liquid feedstock for integrated fuel processors with reforming in supercritical water.

6.3 THERMODYNAMICS OF SCWG

6.3.1 Chemical Reactions

The high-temperature SCWG of organic species is a very complex process, and various competing chemical reactions can occur. The reaction pathways focus on reactions involving gas species. The main reactions in SCWG are the SR reaction, WGS reaction, pyrolysis reaction, and methanation reaction [60,86,91–95]. Partial oxidation reactions can also occur in the presence of oxygen. When complex-structured feedstocks such as lignocellulosic biomass are used, the first step is the solvation of biomacromolecules that occurs simultaneously with hydrolytic attacks on the macromolecular structures [96]. For example, cellulose will be hydrolyzed to its monomer (glucose) by the following hydrolysis reaction:

$$(C_6H_{10}O_5)n + nH_2O \rightarrow nC_6H_{12}O_6 \qquad (6.1)$$

Glucose can then undergo a variety of reactions, leading to the formation of reaction intermediates that can be reacted further to form gases.

SR is a highly desirable reaction since it produces hydrogen directly and indirectly through the formation of carbon monoxide (Eqn (6.2)). The SR reaction given below is intended for both hydrocarbon and oxygenated hydrocarbon species. For hydrocarbon, the value of z coefficient is zero.

$$C_xH_yO_z + (x-z)H_2O \leftrightarrow xCO + (x-z+0.5y)H_2 \qquad (6.2)$$

SR is a highly endothermic reaction. For example, in the SR of ethanol and isooctane, the heats of enthalpy (ΔH_{298}) are 256 kJ/mol [86] and 1274.47 kJ/mol, respectively [97]. Higher reaction temperatures will shift the equilibrium in the forward direction and produce higher amounts of hydrogen and carbon monoxide. Hence, high-temperature SCWG is typically applied if hydrogen is the target product, while low-temperature SCWG is favored for the production of methane-rich gases [57,98]. The use of catalysts in SCWG can drive the reaction to the desired product and to decrease the reaction temperature. Rostrup-Nielsen [99] presented

the order of specific activities of a series of catalysts for ethane SR as follows:

$$\mathrm{Rh, Ru} > \mathrm{Ni, Pd, Pt} > \mathrm{Re} > (\mathrm{Ni-Cualloy}) > \mathrm{Co}$$

The SR reaction produced large quantities of carbon monoxide. The WGS reaction can then occur due to the existence of large amounts of water under typical SCWG conditions. This reaction is highly desirable because the forward reaction can produce additional hydrogen.

$$\mathrm{CO + H_2 \leftrightarrow CO_2 + H_2} \tag{6.3}$$

Penninger and Rep [100] showed that the WGS reaction is initiated through the interaction of CO with OH^-, produced by the ionic dissociation of supercritical water, and forms the formate anion ($HCOO^-$). The formate anion then decomposes into carbon dioxide and hydride anion (H^-) according to the following mechanism:

$$\mathrm{OH^- + CO \leftrightarrow HCOO^- \leftrightarrow H^- + CO_2} \tag{6.4}$$

The hydride anion interacts with water to form H_2 and OH^- by electron transfer according to

$$\mathrm{H^- + H_2O \leftrightarrow H_2 + OH^-} \tag{6.5}$$

The catalytic WGS reaction is typically faster than the noncatalytic one in supercritical water [54,63]. The WGS reaction is significantly catalyzed in the presence of alkali salts even at low temperatures (200–400 °C), as reported by Elliot et al. [63]. Various alkali compounds including NaOH, $Na_2C_2O_4$, $Na_2C_2H_3O_2$, and $NaHCO_3$ can act as catalysts for the WGS reaction. The order of the WGS reaction activity is alkali metals > transition metals > alkaline earth metals.

If all the feedstocks are steam reformed and all the CO produced by SR is consumed to produce hydrogen, maximum theoretical hydrogen gas yields can be obtained. The combined reaction between SR and WGS reactions is

$$\mathrm{C_xH_yO_z + (2x - z)H_2O \leftrightarrow xCO_2 + (2x + 0.5y - z)H_2} \tag{6.6}$$

Table 6.2 lists the maximum theoretical hydrogen gas yields that can be achieved from various feedstocks when the carbon number is less than eight. When the feedstock is ethanol and isooctane, ΔH_{298} of the combined reaction is 174 kJ/mol [101] and 945.27 kJ/mol [60], respectively. Highly endothermic reactions indicate that higher reaction temperatures are favorable for high hydrogen gas yields.

Other competing reactions such as pyrolysis, methanation, oxidation, boudouard, and hydrogenation can also occur during SCWG. The pyrolysis (cracking) reaction is endothermic, but it is considerably less endothermic than reforming reaction [91]. The pyrolysis

TABLE 6.2 Theoretical Maximum Hydrogen Gas Yields of Several Feedstocks

Feedstock	Formula ($C_xH_yO_z$)	Theoretical Hydrogen Yield ($2x + 0.5y - z$)
Methane	CH_4	4
Methanol	CH_4O	3
Ethanol	C_2H_6O	6
Glycerol	$C_3H_8O_3$	7
Glucose	$C_6H_{12}O_6$	12
Isooctane	C_8H_{18}	25

reaction is considered to be responsible for the formation of coke, tar, and gaseous hydrocarbons. Methane can be produced by the reaction of carbon monoxide, carbon dioxide, or carbon with hydrogen. The methanation of carbon monoxide is given as follows:

$$\mathrm{CO + 3H_2 \leftrightarrow CH_4 + H_2O}$$
$$\Delta H_{298\ \mathrm{K}} = -206.17\ \mathrm{kJ/mol} \tag{6.7}$$

The methanation of carbon dioxide is

$$\mathrm{CO_2 + 4H_2 \leftrightarrow CH_4 + 2H_2O}$$
$$\Delta H_{298\ \mathrm{K}} = -165.01\ \mathrm{kJ/mol} \tag{6.8}$$

The methanation of carbon is

$$\mathrm{C + 2H_2 \leftrightarrow CH_4} \quad \Delta H_{298\ \mathrm{K}} = -74.87\ \mathrm{kJ/mol} \tag{6.9}$$

Because hydrogen produced by SCWG is consumed by the methanation reactions, it is not desirable. All the methanation reactions are exothermic, and it can be avoided by running SCWG at high temperatures or removing the methane continuously from the reactor. The methanation of carbon monoxide and carbon dioxide can be catalyzed by ruthenium, iridium, rhodium, nickel, cobalt, osmium, platinum, iron, palladium, molybdenum, or silver [102,103].

In the presence of oxidants, partial oxidation reaction (Eqn (6.10)) or total oxidation reaction (Eqn (6.11)) can occur, depending on the amount of oxidant.

The partial oxidation reaction is given as follows:

$$\mathrm{C_xH_yO_z + (x - z)/2O_2 \leftrightarrow xCO + 0.5\,yH_2} \tag{6.10}$$

The total oxidation reaction is given by

$$\mathrm{C_xH_yO_z + (2_x + 0.5_{y\,-\,z})/2O_2 \leftrightarrow xCO_2 + 0.5\,yH_2O} \tag{6.11}$$

Carbon monoxide generated from the partial oxidation reaction can react with water using the WGS reaction

to produce hydrogen. The oxidation reactions are exothermic, and hence, the presence of oxidants can lead to internal heating, thereby reducing the external energy required for SR reactions. In addition, the oxidation reaction can reduce the formation of the coke or tar by gasifying it to a gaseous product [88,104].

Several reactions are responsible for the carbon formation through reaction intermediates, for instance char formation [96].

$$C_xH_yO_z \leftrightarrow wC + C_{x-w}H_yO_z \quad (6.12)$$

The boudouard reaction is

$$2CO \leftrightarrow C + CO_2 \quad \Delta H_{298\,K} = -172.45\ \text{kJ/mol} \quad (6.13)$$

The negative value of the enthalpy of the boudouard reaction implies that at higher temperatures (T > 680 °C), the endothermic formation of carbon monoxide is the dominant reaction [105].

6.3.2 Estimation of Theoretical Maximum Hydrogen Gas Yield

The theoretical maximum hydrogen gas yields from different feedstocks are different. Based on the assumption that all the feedstocks are reformed to carbon dioxide while the other competing reaction pathways do not disturb the combined SR and WGS reactions, the theoretical maximum hydrogen gas yield that can be achieved is estimated using Eqn (6.6). For example, the theoretical maximum hydrogen gas yield is $(2x + 0.5y - z)$ using a feedstock with the chemical structure of $C_xH_yO_z$. The presence of oxygen (O) in oxygenated hydrocarbons implies that the theoretical maximum hydrogen gas yield is less than that in the case of hydrocarbons with the same number of carbon and hydrogen. Table 6.2 lists the theoretical maximum hydrogen gas yield for several feedstocks.

In the presence of oxidants, partial oxidation or total oxidation reactions can occur depending on the oxidant amount. Under the assumption that the oxygen added is consumed through partial oxidation, all the remaining hydrocarbons are reacted further by the SR reaction, while all the carbon monoxide generated is reacted further through the WGS reaction; the theoretical maximum hydrogen gas yield in the presence of oxygen is then

$$C_xH_yO_z + pO_2 + (2x - z - 2p)H_2O \leftrightarrow xCO_2 + [0.5y + 2(x - p) - z]H_2 \quad (6.14)$$

Here p is the oxygen to steam ratio. Table 6.3 lists the theoretical maximum hydrogen gas yield for glucose for different oxidant amounts.

TABLE 6.3 Theoretical Maximum Hydrogen Gas Yields of Glucose in the Presence of Oxidant

Feedstock ($C_xH_yO_z$)	Oxygen to Hydrocarbon Ratio (p)	Theoretical Hydrogen Yield ($0.5y + 2(x - p) - z$)
Glucose ($C_6H_{12}O_6$)	0	12
	0.1	11.8
	0.5	11
	1	10
	2	8

6.3.3 Optimization of Operation Parameters

The main chemical reactions of SCWG, such as SR, WGS, and methanation, are reversible reactions. Hence, to achieve the maximum hydrogen gas yield, the operating parameters (temperature, pressure, reactant ratio, residence time, and catalysts) must be optimized. The SCWG performance is typically evaluated using parameters such as total gas yield, individual gas yield, and carbon gasification efficiency (CE). The total gas yield is defined as the number of moles of each produced gas per mole of the feedstock fed to the reactor. The individual gas yield (e.g. hydrogen gas yield) is defined as the number of moles of the produced gas per mole of the feedstock fed to the reactor. The CE is defined as the total number of moles of carbon in the produced gases per the total number of moles of carbon in the feed. The CE is a type of carbon balance that is used due to the difficulties in achieving mass balance for solid products that may remain in the reactor.

6.3.3.1 Temperature

The reaction temperature is an important parameter that affects the efficiency of the gasification reaction. The combined SR and WGS reactions are highly endothermic, and hence, high external energy is required to drive the equilibrium reaction to form hydrogen and carbon dioxide. Based on Le Chatelier's principle, high temperatures shift the equilibrium of the endothermic reaction in the forward direction (Eqn (6.6)), while lower reaction temperatures are favored for methane production (Eqns 6.7–6.9). Hence, at high reaction temperatures, hydrogen formation predominates over methane formation. The experimental results reported in the SCWG of methanol [92], ethanol [101], glycerol [87,88], and glucose [88] agree well with the above principle. For example, during the gasification of methanol at 276 bar, the hydrogen gas yield increases from ~0.2 to ~1.3 mol/mol methanol as the temperature increases from 500 °C to 700 °C [92]. In ethanol gasification at

221 bar, the hydrogen gas yield increases from ~2.5 to ~3.6 mol/mol ethanol and the methane yield decreases from ~0.75 to ~0.6 mol/mol ethanol as the temperature increases from 600 °C to 800 °C [101]. High temperatures are also favored at higher carbon gasification efficiency (CE) [106] and less severe coke formation because supercritical water becomes a more powerful reactant as the temperature increases [106]. The kinetic rate constant and reaction rate increase with temperature, leading to higher conversions of feedstocks.

The equilibrium gas yield calculation based on Gibbs free energy minimization method with the Peng–Robinson or Soave–Redlich–Kwong equation can predict the product compositions at a specific temperature, pressure, and feedstock concentration. Figure 6.2 shows the equilibrium product composition of 1.8 wt% glucose gasification at a fixed pressure of 250 bar as a function of the temperature (200–800 °C). When the temperature is increased, hydrogen and carbon dioxide gas yields increase, while methane gas yield decreases. From the equilibrium gas yield estimations, it is possible to determine the optimum reaction temperature that leads to high hydrogen gas yields. For example, the hydrogen yield seems to be nearly constant after 650 °C, and operations at temperatures higher than 650 °C will be ineffective.

6.3.3.2 Pressure

Based on Le Chatelier's principle, increasing pressure will shift the equilibrium reactions toward the side of fewer molecule formations. Hence, a decrease in the pressure can lead to an increase in carbon dioxide and hydrogen products (Eqn (6.6)) and to a decrease in the methane product (Eqns 6.7–6.9).

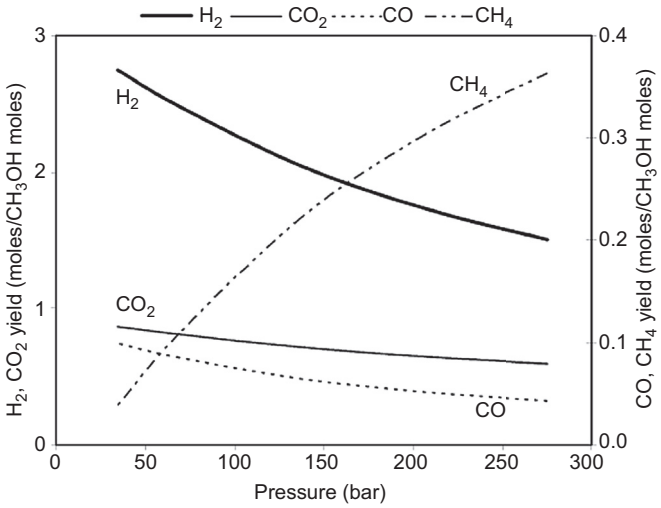

FIGURE 6.3 Equilibrium gas yield as a function of pressure in the gasification of 10 wt% methanol at 700 °C. *Reprinted with permission from Ref. [107].*

Figure 6.3 shows the equilibrium gas yield as a function of pressure estimated from the Gibbs free energy minimization for 10 wt% methanol gasification at 700 °C. As the pressure increases from 34 bar to 276 bar, the hydrogen gas yield decreases from ~2.8 to ~1.5 mol/mol methanol and carbon dioxide gas yield decreases from ~0.8 to ~0.7 mol/mol methanol, while methane gas yield increases significantly from ~0.04 to ~0.37 mol/mol methanol. Further, the experimentally observed pressure effects on individual gas yields agree well with the theoretically estimated gas yields. Gadhe et al. [107] demonstrated that pressure had a negative effect on the hydrogen gas yield in SCWGs with 10 wt% methanol at 700 °C. The hydrogen gas yield decreased from 2.75 mol/mol methanol at 34 bar to 1.5 mol/mol methanol at 276 bar. Under this condition, the methane gas yield increased from 0.03 to 0.24 mol/mol methanol, while the carbon monoxide gas yield decreased from ~0.9 to ~0.3 mol/mol methanol and carbon dioxide gas yield decreased from ~1.0 to ~0.6 mol/mol methanol as the pressure increased from 34 to 276 bar. The significant dependence of pressure on the individual gas yields may be because of the competition between the free radical reaction and ionic reaction with changes in the density with pressure. The free radical reaction decreases with increase in the pressure as a result of the cage effect, while ionic reactions increase with pressure because of ionic compounds' stabilization at higher densities. The gaseous products are typical products of the free radical reaction [31].

It is to be noted that over a narrow range of pressure changes in the supercritical state (e.g. 221–276 bar), pressure has negligible effects on the hydrogen gas yield. For example, in the SCWG of 10 wt% ethanol at 700 °C, the hydrogen gas yield changed marginally from ~2.54 to ~2.64 mol/mol ethanol when the pressure increased from 221 to 276 bar [101].

6.3.3.3 Feedstock Concentration

In a typical SCWG, the feedstock concentration has a significant impact on the individual gas yields. When low feedstock concentrations are used, the large amount of water can shift the WGS reaction (Eqn (6.5)) in the forward direction. This can lead to increases in the hydrogen and carbon dioxide gas yields. In addition, excess water conditions can shift the methanation reactions (Eqns 6.7 and 6.8) in the backward direction, thereby leading to decreasing methane gas yields.

The equilibrium calculations in Figure 6.4 show that when the feedstock concentration increases, the hydrogen gas yield decreases significantly and carbon dioxide gas yield decreases slightly, while methane and carbon monoxide gas yields increase. Thus, at low feedstock concentrations, hydrogen and carbon dioxide

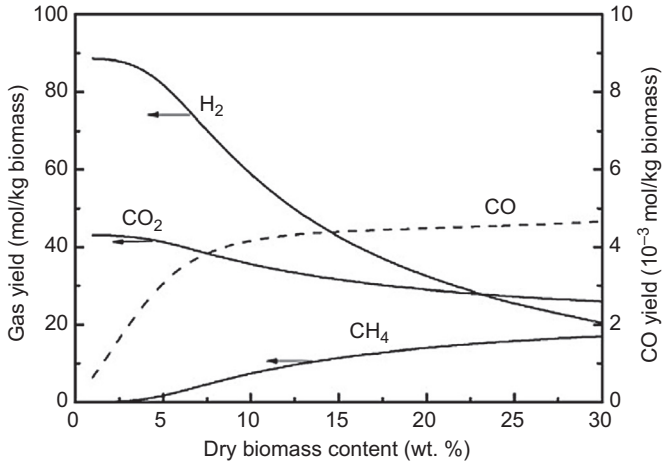

FIGURE 6.4 Equilibrium gas yield as a function of concentration in the gasification of biomass at 600 °C and 250 bar. *Reprinted with permission from Ref. [156].*

are the dominant gaseous products, while at high concentrations, carbon monoxide and methane production are remarkable. Low feedstock concentrations are preferable for higher hydrogen gas yields, while high feedstock concentrations are desirable for higher hydrogen productivity. This principle is proved from the experimental gasification results for methanol [107], glycerol [87], and glucose [108].

6.3.3.4 Residence Time

The effects of residence time on the individual gas yields depend significantly on other reaction parameters such as temperature, pressure, feedstock concentration, feedstock species, and reactor design. Short-chain hydrocarbon or oxygenated hydrocarbon species typically require relatively shorter residence times than longer chain hydrocarbons for complete conversions. For example, when 5 wt% glycerol was gasified at 800 °C and 241 bar, an increase in the residence time from 1 to 2 s resulted in a decrease in the hydrogen gas yield from 6.5 mol H_2/mol glycerol to 3 mol/mol glycerol. Considerably longer residence times (>100 s) were required to achieve maximum hydrogen gas yields at ~765 °C when long-chain hydrocarbons such as isooctane and jet propellant (JP) fuel were used as the feedstocks. In this manner, depending on the feedstock properties (chain length, chemical structure, and oxygen content), the optimum residence times to achieve maximum hydrogen gas yields are different [107]. When SCWG is operated beyond the optimum residence time, enhanced methanation activity can either decrease the hydrogen gas yield [95,101,107] or the product composition remains unchanged [93]. For example, in the residence time investigations, Gadhe et al. [107] fixed the flow rate but changed the reactor length in order to avoid possible interventions of the flow patterns in the reactor. They reported that the 1-m-length reactor had better hydrogen gas yields than those from the 0.5- and 2-m-length reactors in the case of 1 ml/min feed of 10 wt% methanol at 276 bar and 700 °C. Boukis et al. [93] showed that the individual gas yields of hydrogen, carbon dioxide, carbon monoxide, and methane did not change when the residence time increased from 40 up to 100 s in the SCWG of 26.2 wt% methanol at 250 bar and 400 °C. At the higher temperature of 500 °C, the hydrogen gas yield was independent of the residence time up to 54 s. When the temperature increased to 600 °C, the hydrogen gas yield decreased as the residence time increased due to the enhanced methanation reaction. Operations at higher reaction temperatures [101] or catalyst utilization [108] can typically shorten the residence time required to achieve complete conversion.

6.4 GASIFICATION OF SIMPLE FEEDSTOCKS

6.4.1 Methanol

Methanol (CH_3OH) is the simplest feedstock that has been extensively tested in SCWG. Methanol contains C, H, and O atoms, all of which are the main components of a typical biomass. Further, methanol can be produced from a variety of sources including natural gas, coal, and biomass (wood waste, agriculture residue, and garbage). Methanol was the first fuel from wood and is often called "wood alcohol". Methanol has high hydrogen to carbon ratio (H/C = 4), which enables the achievement of high yields of hydrogen per mole of feed. The theoretical maximum hydrogen gas yield using methanol as the feedstock is 3 mol H_2/mol methanol. The absence of carbon–carbon bond in methanol enables the gasification reactions to be conducted at relatively lower temperatures than those of longer chain feedstocks [92]. Moreover, the requirement to produce hydrogen onboard makes methanol a promising hydrogen source due to the ease of storage and transport [109].

The results for the SCWG of methanol are summarized in Table 6.4. Note that the experimentally determined hydrogen gas yield often exceeds the estimated equilibrium hydrogen gas yield. This may be due to either the enhanced activity of WGS reactions under the given experiment conditions [55] or the simpler structures of methanol that make gasification easier even in the absence of a catalyst. However, the experimentally determined hydrogen gas yield has not reached the theoretical maximum hydrogen gas yield of 3 mol/mol methanol, even though some catalysts were used and gasification was conducted at the high temperature of 700 °C.

TABLE 6.4 Summary of SCWG Experiment Results and Theoretical Hydrogen Gas Yields Using Methanol (CH_3OH) as a Feedstock

Catalysts	Reactor Types (Reactor Material)	Experiment Conditions	CE (%)	Theoretical Max H_2 Yield (mol H_2/mol CH_3OH)	Equilibrium H_2 Yield (mol H_2/mol CH_3OH)	Experimental H_2 Yield (mol H_2/mol CH_3OH)	Refs
No	Continuous tubular reactor (Inconel 625)	345 bar; 600 °C; ~3.2 wt%, Weight Hourly Space Velocity (WHSV) = 0.54/h	79	3	1.65	2.17	Xu et al., 1996 [68]
Coconut shell AC			84			2.13	
No	Continuous tubular reactor (Inconel 625)	250 bar; 600 °C; 26.2 wt%; ~4 s	NA[2]		0.363	~2.55	Boukis et al., 2003 [93]
No	Continuous tubular reactor (Inconel 625)	250 bar; 600 °C; 26.2 wt%; 16 s	93%		0.363	~2.4	Boukis et al., 2006 [110]
No	Continuous tubular reactor (Inconel 600)	276 bar; 700 °C; 10 wt%; 29.4 s[1]	NA[2]		1.5	~2	Gadhe et al., 2005 [107]
0.68 wt% K_2CO_3						~2.43	
0.83 wt% KOH						~2.77	
No	Continuous tubular reactor (Inconel 625)	276 bar; 700 °C; 15 wt%; 6 s	NA[2]		1.1	H_2 composition (~72%)	Taylor et al., 2003 [59]

[1]*Calculated based on the literature information.*
[2]*Not available.*

In 1996, Prof. Antal's group reported that SCWG of ~3.2 wt% of methanol yielded 2.17 mol H_2/mol of methanol without the use of catalysts at 600 °C and 345 bar [68]. Approximately 72% of the theoretical maximum hydrogen yield was achieved at the low temperature. The carbon gasification efficiency was ~79%. The SCWG using coconut shell-AC catalyst showed similar hydrogen gas yields of 2.13 mol H_2/mol methanol, but higher carbon gasification efficiency (84%). A more detailed investigation into the SCWG of methanol was conducted by the Boukis' group using both laboratory-scale and pilot-scale apparatus [93,110]. A set of laboratory experiments was carried out at 600 °C and 250 bar by varying the initial feed concentrations using an Inconel 625 reactor. High conversions (~99%) up to 50 wt% concentration were achieved when the gasification was conducted with residence times longer than 4 s, while the conversion decreased dramatically at feed concentrations higher than 50 wt%. At the concentration of 15 wt% in the absence of catalyst, the hydrogen gas yield was ~2.5 mol/mol methanol. The pilot-scale experiments, which were conducted at 580 °C, 280 bar, 13.5 wt%, and total flow rate of 95 kg/h, confirmed the results of the laboratory-scale experiments; almost complete conversion of 99% was achieved. The composition of the produced gases was 72.4% H_2, 20.8% CO_2, 4.4% CH_4, and 3.1% CO. Trace amounts of methanol and organic acid (formic acid and acetic acid) were found in the liquid effluent. Tar formation was not detected. Gupta's group focused on a strategy to suppress methane production during the SCWG of methanol [107]. The methane formation was suppressed by operating the SCWG with low residence times, by adding base or alkali catalysts, or by utilizing the surface catalyst effects of the reactor made of Inconel 600 (Ni–Cu alloy). They observed that the hydrogen gas yields decreased at higher pressures, longer residence times, and low steam to carbon ratios. At 276 bar, 700 °C, 10 wt% feed, and feed flow rate of 1 ml/min (~29.4 s), the hydrogen gas yield was ~2 mol/mol methanol in the absence of catalysts, while the hydrogen gas yield was ~2.7 mol/mol methanol when 0.83 wt% KOH was used as the catalyst. Taylor et al. [59] also investigated different hydrocarbon reformings in supercritical water using a tubular Inconel 625 reactor at 276 bar and 550–700 °C. Their results showed that at 700 °C and 276 bar, complete methanol conversions were achieved at methanol concentrations of 25 wt% or less for all the investigated residence times (3–6 s) and for concentrations of 35 wt% at 6 s only. Hydrogen in the gaseous product was ~72% at 10 wt%, and it decreased gradually to 65% when the concentration increased to 45 wt%.

6.4.2 Ethanol

Ethanol is an attractive feedstock as a source of hydrogen for several reasons: (1) it contains relatively high hydrogen content (H:C = 3:1), (2) it is nontoxic and biodegradable, (3) it is easy to store and transport, and (4) more importantly, it can be produced from

renewable biomass sources such as corn, lignocellulosic biomass, and energy crops by fermentation [2,111,112]. The ethanol produced from the biomass is called bioethanol. After fermentation, the produced ethanol contains large amounts of water (~12 wt%) [112]. A highly energy-intensive process is thus required to remove the water that is to be used in combustion transportation engines as a gasohol (mixture of gasoline and ethanol). The energy required for distillation and drying—in order to volatilize the water remaining in fermented ethanol—is approximately 50% of the total energy consumed to produce corn ethanol [113]. Bioethanol with excess water can be a potential feedstock for hydrogen production via gasification in supercritical water because water evaporation can be avoided. This can save the cost of dealing with the separation of water via distillation and drying. The hydrogen efficiency from corn ethanol in fuel cells is considerably higher (~60%) than that when it burns in a combustion engine (~20%) [114,115]. Ethanol can be regarded as a simple model compound for wet biomass since it contains both carbon−carbon and carbon−oxygen bonds [116].

There are only a few reports on the gasification of ethanol in supercritical water. Table 6.5 summarizes the results of the SCWG of the ethanol, which have been obtained thus far. The theoretical maximum hydrogen gas yield is 6 mol/mol ethanol. In 2002, the noncatalytic gasification of ethanol in supercritical water at relatively low temperatures has been investigated using a flame-sealed small quartz tube to avoid wall catalytic effects [117]. The experiment was conducted at a temperature of 500 °C and density of 0.2 g/cm^3 (~430 bar). The produced gases contain H_2, CH_4, CO, CO_2, C_2H_6, and C_2H_4, and the only gas detected in the liquid product was acetaldehyde. Further heating led to the decomposition of acetaldehyde to gaseous products (CH_4 and CO) without the formation of acetic acid. The hydrogen gas yield was low (~1.2 mol% at 450 °C and 30 min; ~23 mol% at 500 °C and 60 min). The reaction pathway of noncatalytic ethanol reforming in supercritical water was proposed by Arita et al. [117] as follows: (1) dehydrogenation of ethanol to CH_3CHO, (2) decomposition of CH_3CHO to CH_4 and CO, and (3) conversion of CO to H_2 by the WGS reaction. The decomposition of ethanol in the absence of catalyst under the present experimental conditions may have three possible mechanisms—ion-, radical-, and water-catalyzed mechanisms. They concluded that the water-catalyzed mechanism appears to be the most reasonable but further evidence is required. Taylor et al. [59] investigated the SCWG of ethanol with 276 bar and 700 °C and residence times of 3 and 6 s using a tubular Inconel 625 reactor. Their results showed that the gasification conversion of 15 wt% ethanol was significantly lower than that of methanol under identical conditions. The compositions of hydrogen gas, methane, and CO were less than 50%, ~25%, and ~3%, respectively, while that of ethane was less than 1% for a residence time of 6 s.

The catalytic effects of ethanol reforming in supercritical water were investigated by Byrd et al. [101] The hydrogen gas yield increased from 3 to 4.5 mol/mol ethanol when 5 wt% Ru/Al_2O_3 catalyst at 10 wt%, 800 °C, 221 bar was added with a residence time of 4 s using a tubular Inconel 600 reactor. In the absence of a catalyst, the hydrogen gas yield is less than equilibrium hydrogen gas yield (3.98 mol/mol ethanol), while the catalyst utilization can drive the hydrogen gas yield to over 100% of the equilibrium value due to the enhanced WGS reaction. By decreasing the feedstock concentration to 5 wt%, further increases in the hydrogen gas yields to 5.3 mol/mol ethanol (hydrogen composition in the dry gas composition was 73%) were obtained. This value is

TABLE 6.5 Summary of SCWG Experiment Results and Theoretical Hydrogen Gas Yields Using Ethanol (C_2H_5OH) as a Feedstock

Catalysts	Reactor Types (Reactor Material)	Experiment Conditions	CE (%)	Theoretical Max H_2 Yield (mol H_2/mol C_2H_5OH)	Equilibrium H_2 Yield (mol H_2/mol C_2H_5OH)	Experimental H_2 Yield (mol H_2/mol C_2H_5OH)	Refs
No	Batch (Quartz tube)	0.34 g/cm^3 (~447.8 bar[1]); 450 °C; ~3.2 wt%; 30 min	NA[2]	6	0.26	NA[2] (H_2 = ~1.2 mol %)	Arita et al., 2003 [117]
No	Continuous tubular reactor (Inconel 625)	276 bar; 700 °C; 15 wt%; 6 s	NA[2]		1.66	NA[2] (H_2 = 48% mol)	Taylor et al., 2003 [59]
No	Fixed bed tubular reactor (Inconel 600)	221 bar; 80 0 °C; 10 wt%; 4 s	NA[2]		3.98	3	Byrd et al., 2007 [101]
Ru/Al_2O_3		221 bar; 800 °C; 10 wt%; 4 s			3.98	4.5	
		221 bar; 800 °C; 5 wt%; 4 s			5.36	5.3	

[1]*Calculated based on supercritical water properties.*
[2]*Not available.*

very close to the hydrogen gas yield at equilibrium (5.36 mol/mol hydrogen) and approximately 88% of the theoretical maximum (6 mol/mol ethanol). Methane formation was significantly suppressed by the addition of the Ru catalyst with conversions greater than 99%.

Rabe et al. [116] proposed the ethanol reforming mechanism during SCWG in the presence of a Ru/carbon catalyst using a capillary tube reactor. At around 250 °C, ethanol absorbs on the Ru catalyst and decomposes to CH_3CHO (acetaldehyde) and hydrogen as follows:

$$C_2H_5OH \rightarrow CH_3CHO + H_2 \quad (6.15)$$

Acetaldehyde accumulates on the catalyst surface to a certain extent because its formation is faster than its decomposition to methane or carbon monoxide.

$$CH_3CHO \rightarrow CO + CH_4 \quad (6.16)$$

The carbon monoxide formed is strongly adsorbed and reacts quickly with the surrounding water through the WGS reaction to form hydrogen (Eqn (6.7)) and carbon dioxide that may further hydrogenate to form methane (Eqn (6.8)). At higher temperatures of 350 °C, CO_2 may also be formed from the decarboxylation of another surface intermediate, presumably from acetaldehyde. They concluded that ethanol decomposition over the Ru/C catalyst was complete at above approximately 350 °C. At this temperature, the gas composition was 70% CH_4, 17% CO_2, and 3% H_2. The ruthenium catalyst remained fully reduced during the subcritical and supercritical gasification reactions, and this was confirmed by X-ray absorption near-edge spectroscopy. The formation of reactive intermediates such as acetaldehyde in the ethanol reforming, which reacts further to form CO_2 and H_2, has also been observed by other researchers [118,119]. Schanzenbacher et al. [120] observed that acetaldehyde is the only liquid product from the hydrolysis of ethanol, while formaldehyde and acetic acid were found along with acetaldehyde during the ethanol oxidation at 433–494 °C and 246 bar.

More investigations and optimizations for ethanol reforming in supercritical water are still required. Even though the hydrogen gas yield almost reached the theoretical maximum value (~88%), the utilization of catalysts at high temperatures and low feedstock concentrations are considered to be unprofitable. Long-term catalytic stability in the case of the ethanol reforming in supercritical water also needs investigation.

6.4.3 Glucose

Hydrogen reforming from glucose in supercritical water has been extensively studied. The solvolysis study of six woody and four herbaceous biomass species at 200–230 °C for 0–15 min showed that almost 100% of the hemicellulose was soluble in high-temperature water, and 90% (on an average) can be recovered as monomeric sugar species [121]. Cellulose is a polysaccharide consisting of hundreds or thousands of β(1 → 4) linked D-glucose units. Consequently, glucose serves as a good model compound of cellulose and hemicellulose.

In the mid-1970s, Prof. Modell's group investigated glucose gasification in supercritical water at 218 bar and 374 °C. High glucose conversions (~100%) were obtained, but the hydrogen gas yield was low since glucose was converted to reaction intermediates in the liquid phase [122]. Subsequently, in 1993, Yu et al. [52] reported that almost complete gasification of glucose was achieved at 600 °C, 345 bar and residence time of 34 s using tubular Inconel 625 and Hastelloy C276 reactors when a low glucose concentration of ~1.8 wt% was used. The gasification efficiency measured by carbon balance was >90%. At higher feed concentrations of 7.2–14.4 wt%, the gasification efficiency decreased to 68–85%. The hydrogen gas yields were 7.7–8.2 mol/mol glucose at the low glucose concentrations of 1.8–3.6 wt%, which approached the equilibrium yield (6.92–10.2 mol/mol glucose). As listed in Table 6.6, the hydrogen yield decreased to 0.56 mol/mol glucose at a high concentration of 21.6 wt%, which is considerably lower than the equilibrium value [68]. Hydrogen and carbon dioxide were the main gaseous compounds at the low glucose concentration of 1.8 wt%, while carbon monoxide was the predominant gaseous composition at the high concentration of 14.4 wt%. For example, in the experiments conducted in the Inconel reactor, hydrogen and carbon dioxide were ~62 mol% and ~30% mol, respectively, at a concentration of 1.8 wt%, while carbon monoxide was ~43 mol% at the concentration of 14.4 wt% [52]. In addition, they reported the catalytic effects of the reactor wall on the glucose reforming. The Inconel 625 and corroded Hastelloy C276 reactor seemed to catalyze the WGS reaction (Eqn (6.7)), thereby producing gases that are rich in hydrogen and carbon dioxide. Higher carbon efficiencies and carbon monoxide compositions were obtained with a new Hastelloy C276, presumably due to enhanced SR reactions (Eqn (6.2)). Even though glucose gasification at low concentrations showed that complete gasification with high hydrogen gas yields can be achieved, higher feed concentrations have to be handled to enhance hydrogen productivity. Hao et al. [123] reported that 7.2 wt% glucose was completely gasified at 650 °C, 250 bar, and 3.7 min using a stainless-steel tubular reactor. Nevertheless, the hydrogen composition in the gas product was small. The gas composition was hydrogen (19.3%), carbon dioxide (29.7%), carbon monoxide (29.9%), methane (16.1%), ethane (4.3%), and ethylene (0.7%). Lee et al. [124] reported that 10.8 wt%

glucose was completely gasified to gaseous products when the reaction temperatures increased to750 °C at 280 bar using a Hastelloy C276 tubular reactor. The hydrogen gas yield at 10.8 wt% and 30-s residence time was 7 mol/mol glucose, which is very close to the equilibrium value (7.85 mol/mol glucose). The major gaseous composition was hydrogen (~55%) and carbon dioxide (~32%), while the minor composition was

TABLE 6.6 Summary of SCWG Experiment Results and Theoretical Hydrogen Gas Yields Using Glucose ($C_6H_{12}O_6$) as a Feedstock

Catalyst	Reactor Types (Reactor Material)	Experiment Conditions	CE (%)	Theoretical Max H_2 Yield	Equilibrium H_2 yield	Experimental H_2 Yield	Refs
				(mol H_2/mol $C_6H_{12}O_6$)			
No	Continuous tubular reactor	345 bar; 600 °C; ~3.6 wt%; 34 s	82	12	6.92	6.3	Yu et al., 1993 [52]
	Inconel 625	345 bar; 600 °C; ~1.8 wt%; 34 s	~90		10.2	~8.2	
	Corroded Hastelloy	345 bar; 600 °C; ~3.6 wt%; 34 s	86		6.92	7.7	
	New Hastelloy	345 bar; 600 °C; ~3.6 wt%; 34 s	89		6.92	1.8	
No	Continuous tubular reactor Inconel 625	345 bar; 600 °C; ~21.6 wt%; 34 s	80		1.42	0.56	Xu et al., 1996 [68]
Coconut shell AC		WHSV 22.2/h	103			2.24	
Coal AC		WHSV 19.9/h	97			1.48	
Macadamia shell charcoal		WHSV 25.7/h	95			2.71	
Spruce wood charcoal		WHSV 12.6/h	99			3.86	
KOH	Continuous tubular reactor	250 bar; 600 °C; ~3.6 wt%; 30–120 s	>96		8.42	9.1	Schmieder et al., 2002 [86]
	Inconel 625						
No	Continuous tubular reactor	280 bar; 750 °C; 10.8 wt%; 30 s	99.7		7.85	~7	Lee at al., 2002 [124]
No	Bomb reactor (batch) SS316	0.2 g/cm^3 (~330 bar[1]); 440 °C; 0.3 g glucose; 10 min	NA[4]		Feedstock concentration NA[4]	~0.24[2]	Watanabe et al., 2002 [126]
ZrO_2						~0.6[2]	
NaOH						~3[2]	
No	Continuous tubular reactor	250 bar; 650 °C; ~7.2 wt%, 3.7 min	89.7		6.98	HYP[3]	Hao et al., 2003 [123]
	Stainless steel					(100.8%)	
No	Batch (autoclave)	300 bar; 500 °C; 5 wt %; 1 h; heating rate of 3 K/min	NA[4]		2.4	~1.68	Sinag et al., 2004 [157]
0.5 wt% K_2CO_3	Inconel 625					~1.93	
No	Continuous tubular reactor	248 bar; 700 °C; 1 wt%, 2 s	NA[4]		11.94	~6.5	Byrd et al., 2007 [108]
	Inconel 600	248 bar; 700 °C; 1 wt%,~4 s				~7.25	
Ru/Al_2O_3		248 bar; 700 °C; 1 wt%, 2 s				~12	

TABLE 6.6 Summary of SCWG Experiment Results and Theoretical Hydrogen Gas Yields Using Glucose ($C_6H_{12}O_6$) as a Feedstock—cont'd

Catalyst	Reactor Types (Reactor Material)	Experiment Conditions	CE (%)	Theoretical Max H_2 Yield (mol H_2/mol $C_6H_{12}O_6$)	Equilibrium H_2 yield (mol H_2/mol $C_6H_{12}O_6$)	Experimental H_2 Yield (mol H_2/mol $C_6H_{12}O_6$)	Refs
No	Microchannel reactor SUS 316	250 bar; 750 °C; 1.8 wt%; 2.6–26.3 s	81 ± 3.4		11.9	5.7 ± 0.3	Goodwin et al., 2008 [130]
No	Hastelloy C276	280 bar; 725 °C; 10.8 wt%; 12/h LHSV	~99–100		7.09	~3.5	Lee et al., 2009 [125]
Ni/AC						~5.5	
No	Continuous tubular reactor Haynes® 230®	250 bar; 767 °C; 1.8 wt%; 60 s	91		11.9	11.5	Susanti et al., 2012 [131]

[1]*Calculated based on physical properties of water.*
[2]*Converted from H_2 yield (mol%) to mol H_2/mol glucose based on the definition provided in the paper.*
[3]*HYP: sum of measured hydrogen and hydrogen that could be theoretically formed by completely shifted CO and reform hydrocarbon.*
[4]*Not available.*

carbon monoxide (~5%) and methane (~8%). Lee et al. also reported significantly different results with similar experimental conditions and identical reactor system [124,125]. They suggest that changes in the reactor wall due to aging might affect the gas yield.

The catalytic wall effects led to further investigations on the catalytic role in glucose gasification using heterogeneous catalysts such as AC [68,125], ZrO_2 [126], Ru/Al_2O_3 [108], and Ni/AC [125], and homogeneous catalysts such as NaOH [127], K_2CO_3 [128,129], KOH [86,123], and Na_2CO_3 [123]. The role of catalysts can be summarized as follows: (1) the rate of biomass decomposition with respect to reaction intermediate can be enhanced, (2) WGS reaction can be promoted, and (3) methanation reaction can be suppressed. The gasification efficiency and hydrogen gas yield can thus be improved by utilizing catalysts.

The AC catalyst dramatically increased the CE and decreased the CO content in the gaseous product [68]. The catalytic SCWG of concentrated glucose solutions (21.6 wt%; Table 6.6) using the AC catalysts showed that almost compete gasification efficiency and high hydrogen gas yields of 1.48–3.86 mol/mol glucose can be obtained. These hydrogen gas yields are higher than the equilibrium hydrogen gas yields (1.42 mol/mol glucose). Watanabe et al. [126] studied the effects of ZrO_2 and NaOH catalysts on the SCWG of glucose using a stainless-steel (SS316) tube bomb reactor at 440 °C, 10 min, 0.2 g/cm^3, and 0.3 g of glucose. Without the catalyst, the carbon dioxide plus carbon monoxide gas yield was ~13 mol%, while the hydrogen gas yield was ~2 mol% (this corresponds to ~0.24 mol/mol glucose). In the presence of the ZrO_2 catalyst, the carbon dioxide plus carbon monoxide yield was ~17 mol% and the hydrogen gas yield was 5 mol% (~0.6 mol/mol glucose). A considerably higher hydrogen gas yield of 25 mol% (~3 mol/mol glucose) was obtained using the NaOH catalyst when compared to the yield from the ZrO_2 catalyst. The glucose gasification experiments with alkali catalysts such as K_2CO_3 and KOH showed a significant increase in the gasification yield and a decrease in the CO gas content in the produced gases. Schmieder et al. [86] reported that complete gasification was achieved at temperatures higher than 600 °C without the formation of solid or oily by-products under the condition of $1.8–5.0 \times 10^{-3}$ M KOH, 250 bar, 60–140 s reaction time, and 1.8 wt% glucose concentration, thereby forming hydrogen-rich gaseous products. The addition of KOH led to a decrease of more than 20-fold (from 20 vol% to 0.6 vol%) in the CO content. Table 6.6 shows that the average hydrogen yield of 9.1 mol H_2/mol glucose was obtained from a miniature plant at 600 °C, 250 bar, and 3.6 wt% with the addition of 1.8×10^{-3} M KOH. Sinag et al. [128] reported that the hydrogen gas yield increased twice from ~0.87 to ~1.67 mol/mol glucose in the presence of 0.5 wt% K_2CO_3 catalyst at 300 bar, 500 °C, and 1-h reaction time and a heating rate of 1 K/min; on the other hand, at a higher heating rate of 3 K/min, the hydrogen yield increased from ~1.68 to ~1.93 mol H_2/mol glucose. The enhanced WGS reaction in the presence of the alkali catalyst is responsible for the enhanced hydrogen gas yield [86,129]. Byrd et al. [108] reported

that the utilization of 5 wt% Ru/Al_2O_3 catalyst in glucose reforming can lead to almost theoretical maximum hydrogen gas yields of 12 mol/mol glucose and high hydrogen gas compositions of 69% at 700 °C, 248 bar, 2-s residence time, and 1 wt% glucose concentration using a tubular Inconel 600 reactor. This hydrogen gas yield was approximately twice that in the absence of catalyst. The maximum hydrogen yield in the absence of catalyst was achieved at ~4 s and was around 7.25 mol H_2/mol glucose. In the presence of the Ru/Al_2O_3 catalyst, the WGS reaction was enhanced, while methanation reaction was suppressed; this led to higher hydrogen and carbon dioxide gas yields and lower carbon monoxide and methane gas yields than that in the case of noncatalytic SCWG results. However, the hydrogen gas yield decreased from ~12.6 to ~10.8 mol/mol hydrogen as the feed concentration increased from 1 to 5 wt%. Lee et al. [125] showed that the hydrogen gas yield increased from ~3.5 to ~5.5 mol/mol glucose when a 16 wt% Ni/AC catalyst was used at 10.8 wt%, 280 bar, 12/h Liquid Hourly Space Velocity (LHSV), and 725 °C using a tubular Hastelloy C276 reactor.

Table 6.6 summarizes the catalytic and noncatalytic glucose gasification results in supercritical water under various conditions. An increase in the temperature or the use of catalysts can lead to higher CEs and higher hydrogen gas yields [129]. Therefore, it can be concluded that temperatures >600 °C may be required to achieve complete gasification. Meanwhile, experimental hydrogen gas yields could not achieve the theoretical hydrogen yield (12 mol/mol glucose) even at temperatures >750 °C and at concentrations >1 wt % in the absence of a catalyst [108], even though equilibrium calculations showed that the theoretical maximum hydrogen gas yield can be achieved when the temperature is more than 650 °C (see Figure 6.2) at a concentration of 1.8 wt%. For instance, the hydrogen gas yield was 5.7 mol/mol glucose at 750 °C, 250 bar, and 1.8 wt% [130] and was 7.25 mol/mol glucose at 700 °C, 248 bar, and 1 wt% [108]. As listed in Table 6.6, the noncatalytic gasification could achieve 26–91% of the equilibrium hydrogen yield value, except in the case of Yu et al. [52] who could achieve 111% of the equilibrium hydrogen yield using a corroded Hastelloy C276 reactor. The use of catalysts increased the hydrogen gas yield and hydrogen amounts in the product gas. For example, the hydrogen content in the gas product significantly increased from 54 to 69 mol% in the presence of the Ru/Al_2O_3 catalyst [108]. Recently, an equilibrium hydrogen yield was achieved in the set of experiments on glucose gasification in high-temperature supercritical water region without added catalyst. At low concentration of 1.8 wt% glucose, 250 bar, and 767 °C, the hydrogen gas yield was 11.5 wt%, which is very close to the theoretical maximum value (12 mol/mol glucose) [131].

Typical nongaseous products from the SCWG of glucose are char, oily, and/or WSPs, depending on the operating conditions and type of catalyst. The reaction temperature and time had significant effects on the liquid product composition. Moreover, increasing the temperature and reaction time led to less oily and char products. At low reaction temperatures (typically <400 °C), char and oily products were produced [132], while at sufficiently high temperatures, WSPs were the major liquid products. Minowa et al. [66,133–136] studied the product compositions of glucose and cellulose gasification in near-critical and supercritical water. Hydrolysis was the primary step at around 200 °C, and it produced WSPs (mainly sugars); subsequently, further decomposition at around 250 °C produced WSPs (sugar and nonsugar species), gases, oil, and char. The WSPs gasified further to produce gas and oily products, while oily produces were not gasified further, but contributed to char formation. From 330 to 380 °C, at least 47 organic species detected in the oily product by GC/MS at 0 min and 20 organic species persisted at 120 min [132]. The phenolic species increased as the temperature increased from 330 to 380 °C. A similar trend was observed by Sinag et al. at temperatures of 400–500 °C [129]. Holgate et al. [137] detected approximately 26 organic compounds in the liquid effluent from the glucose gasification in supercritical water at 500 °C. The stability of these compounds decreased with increasing temperatures except for the species including 5-hydromethyl furfural and acetaldehyde. These compounds were finally converted to gaseous products. In high-temperature gasification investigation, Goodwin et al. [130] found 23 compounds in the liquid product at 650 °C and 250 bar, and the dominant products were acetic acid, propanoic acid, 2,5-hexanedione, and phenol. At 750 °C, only acetic acid and phenol were identified. They showed that high temperatures were favored for the gaseous formation, which suggests that the WSPs are reaction intermediate products that will be gasified further in supercritical water. Under this condition, higher temperatures appear to suppress the phenolic species formation. The major organic intermediates were acetic acid, propanoic acid, propenoic acid, 2,5-hexanedione, and phenol, whereas the minor organic intermediates were 5-(Hydroxymethyl)furfura (5-HMF), 3-methyl-2 cyclopenten-1-one, and furfural. Many studies have been conducted on the glucose decomposition in subcritical and supercritical water. The mechanism products depend on the operating conditions. Interested readers can note the decomposition of

glucose in subcritical and supercritical water at 650 °C [130] and at 300–400 °C [138].

6.4.4 Glycerol

Glycerol is an odorless colorless viscous liquid that is produced from both natural and petrochemical sources. Recently, a global increase in the production of biodiesel from natural triglycerides has led to the generation of massive amounts of "bioglycerol" as the by-product. Approximately 0.3 kg of crude glycerol is produced for each gallon of biodiesel production [85]. In 2009, the IEA reported that the global production of biodiesel increased by 10-fold from 2000 to 2007 to reach around 8.6 Mt [139]. Approximately 1.5 million tons of glycerol was produced in 2008, while 600,000 tons was produced in 1992 [140]. A large surplus of glycerol is thus generated from the biodiesel plants.

Pure glycerol is a valuable chemical substance that is used in a variety of areas including drugs/pharmaceuticals, personnel care products, foodstuffs, tobacco, and urethane synthesis. However, crude glycerol generated from biodiesel plants has a low value because of numerous impurities. The composition of crude glycerol highly depends on biodiesel production factors such as feed compositions, synthesis processes, and product recovery processes. Typically, crude glycerol contains approximately 50–60% of catalyst residues, salts, soap, unseparated biodiesel (fatty acid methyl esters (FAMEs)), and water. For example, crude glycerol contains methanol (20.8 wt%), glycerol (42.3 wt%), FAMEs (33.1 wt%), moisture (1.52 wt%), and ash (2.28 wt%) [141]. These impurities in crude glycerol hinder its direct use in conventional applications. The most common method to purify glycerol—fractional vacuum distillation—is a highly energy-intensive and costly process; this is the primary reason for treating crude glycerol as a refuse product. The utilization of crude glycerol for hydrogen production using SCWG is a potential alternative to increase its value because organic impurities in crude glycerol have minimal effects on the glycerol gasification. However, it should be noted that the salt solubility in supercritical water is low, and this can cause reactor plugging during the continuous gasification of crude glycerol.

Since the mid-1990s, several studies on pure glycerol reforming in supercritical water have been reported [68,69,142]. Xu et al. reported the SCWG of glycerol with or without AC catalysts using a tubular Inconel 625 reactor [68]. Even though almost complete gasification was achieved in the absence of catalysts at 600 °C, 345 bar, 44 s, and 18.4 wt%, the hydrogen gas yield was considerably lower (3.51 mol/mol glycerol) than that of the theoretical maximum (7 mol/mol glycerol). The carbon catalyst had negligible effects on the gasification, as listed in Table 6.7. Antal et al. [69] showed that the gas product compositions from glycerol gasification depended on the condition of the reactor's wall. At high glycerol concentrations (18.71 wt%), 89–95% carbon gasification efficiency could be achieved in the absence of the reactor wall effect. The hydrogen in the gas product was in the range of 49–52% at 280 bar and 746–758 °C. The carbon deposition in the reactor wall (due to the gasification using other feedstocks) might decrease the hydrogen content to 39–45%. They did not report the hydrogen gas yield. Xu et al. [143] studied the glycerol gasification at relatively lower temperatures of 380–500 °C using a tubular Hastelloy C276 reactor at dilute concentrations of 1 wt%. The hydrogen gas yield increased from ~1.4 to 5.08 mol/mol glycerol as the reaction temperature increased from 380 °C to 500 °C at 250 bar. However, at higher concentrations, hydrogen gas yield decreased significantly, as reported by Chakinala et al. [106]. The hydrogen gas yield was 2 mol/mol glycerol at 10 wt%, 600 °C, and 250 bar.

Higher reaction temperatures that accompanied the catalyst utilization are beneficial for complete glycerol gasification with high hydrogen gas yields. Byrd et al. [87] reported that in the presence of Ru/Al_2O_3 catalyst, which is the same catalyst that was used in ethanol and glucose reforming [101,108], the hydrogen gas yield was up to 6.5 mol/mol glycerol, which is ~93% of the theoretical maximum and ~97% of the equilibrium value at 800 °C, 241 bar, 1 s, and 5 wt%. The gasification experiments over a wide range of concentrations from 5 to 40 wt% at 800 °C showed that the experimental gas yields were very close to the calculated equilibrium gas concentrations, which indicates that the gasification reaction was near its thermodynamic equilibrium. The hydrogen yield increased from 5.1 to 6.5 mol/mol glycerol as the temperature increased from 700 °C to 800 °C and decreased from 6.5 to 2.8 mol/mol glycerol as the residence time extended from 1 s to 2 s. A plugging problem was reported at 700 °C in the continuous glycerol reforming at concentrations higher than 5 wt%, while this problem was resolved by performing gasification at higher temperatures of 800 °C. Typically, hydrogen molar fractions from the glycerol gasification were 50–70% depending on the operating conditions. The liquid products detected in the degradation of glycerol in near-critical and supercritical water were methanol, acetaldehyde, propionaldehyde, acrolein, allyl alcohol, ethanol and formaldehyde, acetic acid, and hydroxyacetone [31,144].

The effects of alkali (Na_2CO_3 [143] and K_2CO_3 [106]) catalysts on glycerol gasification have been examined. An addition of 0.5 wt% K_2CO_3 increased the hydrogen gas yield from 1.84 to 2.7 mol/mol glycerol and decreased the carbon monoxide gas yield from 1.18 to 0.04 mol/mol glycerol at 600 °C, 250 bar, and 10 wt%; this clearly indicates enhanced WGS reactions in the presence of the catalyst [106]. However, Na_2CO_3 had negative effects on

TABLE 6.7 Summary of SCWG Experiment Results and Theoretical Hydrogen Gas Yields Using Glycerol ($C_3H_8O_3$) as a Feedstock

Catalysts	Reactor Type (Reactor Material)	Experiment Conditions	CE (%)	Theoretical Max H_2 Yield	Equilibrium H_2 Yield	Experimental H_2 Yield	Refs
				(mol H_2/mol $C_3H_8O_3$)			
No	Continuous tubular reactor	345 bar; 600 °C; ~18.4 wt%; 44 s	101	7	0.94	3.51	Xu et al., 1996 [68]
Coconut shell AC	Inconel 625	WHSV = 4.36/h	99			3.15	
No	Continuous tubular reactor	280 bar; 746 °C; 18.71 wt%	95%		2.83	NA[1]	Antal et al., 2000 [69]
	Hastelloy C-276					(H_2 = 52 %mol)	
No	Continuous tubular reactor	250 bar; 500 °C; 1 wt%	98%		5.36	5.08	Xu et al., 2009 [143]
0.1 wt% Na_2CO_3	Hastelloy C-276					~1.6	
No	Continuous tubular reactor	250 bar; 650 °C; 10 wt%; 5 s	92		3.01	~2.5	Rabe et al., 2010 [106]
No	Inconel 600	250 bar; 600 °C; 10 wt%; 5 s	66 ± 1.4		2.15	1.84 ± 0.32	
0.5 wt% K_2CO_3		250 bar; 600 °C; 10 wt%; 5 s	100			2.69	
Ru/Al_2O_3	Fixed bed tubular reactor	221 bar; 800 °C; 5 wt%; 1 s	NA[1]		6.68	6.5	Byrd et al., 2008 [87]
	Inconel 600						

[1]*Not Available.*

glycerol gasification. With the addition of 0.1 wt% of Na_2CO_3 at 500 °C, the hydrogen yield decreased dramatically from 5.08 to 1.6 mol/mol glycerol [143]. A detailed reason was not given by the authors.

Even though the SCWG of crude glycerol has clear advantages over other crude glycerol conversion methods, only a few studies have been published. Onwudili et al. [141] reported the gasification of crude glycerol at relatively low temperatures (≤450 °C) with or without the NaOH catalyst in a Hastelloy C batch reactor. At these low temperatures, the oily product dominated (>60 wt%), while the gaseous products were in the range of 3.2–17.5 wt%, depending on the temperature. The hydrogen gas yield was also low (1.49–8.89% mol/mol carbon). The presence of FAMEs in the crude glycerol did not inhibit hydrogen production since they decomposed at temperatures higher than 380 °C. Drastic changes in the product composition were observed in the case of the catalytic reforming of crude glycerol when NaOH was added. As the NaOH concentration increased from 0 to 3 M, the hydrogen composition in the gaseous product increased from 32 to 90 vol% while the carbon dioxide composition decreased from 50 to 8 vol%. The excess amounts of NaOH seemed to participate in the formation of soap from FAMEs and the formation of sodium carbonate (Na_2CO_3) from carbon dioxide. The CO_2-sorbent role of NaOH can drive the WGS reaction in the forward direction, thereby favoring hydrogen production.

More efforts are required to achieve practical utilizations of crude glycerol from biodiesel plants especially in a continuous SCWG system. One of the potential barriers in the SCWG of crude glycerol is plugging that can be caused by the low salt solubility in supercritical water. The high viscosity of crude glycerol (typically around 8.46–8.80 cS depending on the composition [85]) may also cause the pumping problem.

6.4.5 Model Compound for Lignin

Lignocellulosic biomass typically contains 15–25% lignin that is basically aromatic polymers with hydroxyl phenyl propane molecular units connected with ether linkages in a three-dimensional network. Its cross-linked structure containing a highly stable benzene ring chemical structure provides high chemical stability. The decomposition of lignin in supercritical water is initiated by the hydrolysis of the ether linkage, which produces phenolic monomers. Vanillin or catechol has been used as a model compound for lignin in SCWG [83,86]. In fact, vanillin is obtained from softwood lignin, and catechol is found in the hydrolysis of lignin [145].

TABLE 6.8 Summary of SCWG Experiment Results and Theoretical Hydrogen Gas Yields Using a Lignin Model Compound as a Feedstock

Feedstock	Catalyst	Reactor Type (Reactor Material)	Experiment Conditions	CE (%)	Theoretical Max H_2 Yield	Equilibrium H_2 Yield	Experimental H_2 Yield	Refs
					(mol H_2/mol $C_6H_6O_2$)			
Catechol ($C_6H_6O_2$)	0.0018 M KOH	Tubular reactor Inconel 625	200–300 bar; 600 °C; ~2.2 wt %; 30–120 s	NA[1]	13	8.84[2]	10.6	Schmieder et al., 2000 [86]
	0.005 M KOH	Continuous tubular reactor Inconel 625	300 bar; 700 °C; ~6.6 wt%; 60 s	NA[1]		6.35[3]	~6	Kruse et al., 2000 [83]

[1]*Not available.*
[2]*Calculated at pressure of 250 bar.*
[3]*Calculated based on Gibbs free energy minimization method with Peng–Robinson Equation of State (EOS). It is noted that the equilibrium calculation in the paper use EquiTherm program by defining reactions (The value in the paper is ~8) [83].*

There are only a few literature on the gasification of the lignin model compound, as listed in Table 6.8. Schmieder et al. [86] reported vanillin and catechol reforming with or without alkali catalysts using a Inconel 625 tubular reactor. The achievable total organic carbon (TOC) destruction efficiency in the vanillin reforming was more than 99% even in the absence of catalysts. During the gasification of ~2.2 wt% catechol at 600 °C, 200–300 bar, and 30–120 s in the presence of 1.8×10^{-3} M KOH, the hydrogen yield was 10.6 mol/mol catechol. This value is equivalent to ~82% of the theoretical maximum. The hydrogen content was 61.5 vol% and the carbon dioxide content was 29.3 vol% in the gaseous product. The TOC of the effluent liquid was ~20 ppm. Kruse et al. [83] investigated catechol gasification at temperatures ranging from 500 to 700 °C at 200–400 bar using an Inconel 625-lined tumbling batch reactor and an Inconel 625 continuous reactor. The gasification efficiency was in the range of 85–97% and was accelerated at high temperatures. At 500 °C and 250 bar, the addition of 5 wt% KOH enhanced hydrogen content from ~15 to ~50 vol%. The formation of carbon monoxide was significantly suppressed from ~45 vol% to nondetectable contents. The alkaline salt accelerated the WGS reaction as a result of the formation of formates as intermediate products, which subsequently degraded to carbon dioxide and hydrogen. By using the continuous reactor at 700 °C, ~6.6 wt%, 300 bar, and 0.005 M KOH, the hydrogen gas yield reached an equilibrium value of almost ~6 mol/mol catechol after 2-min reaction time. On the other hand, the hydrogen gas yield did not reach equilibrium at 600 °C. These studies have shown that aromatic compounds in biomass can be gasified completely at a high rate in supercritical water, thereby producing hydrogen-rich gaseous products. Alkali salts that are often present in the real biomass can improve the gasification yield and hydrogen production.

6.5 GASIFICATION OF FOSSIL FUELS

Hydrogen production from biomass feedstocks is considered one of the promising renewable energy production pathways that can lessen the dependence of fossil fuels and ameliorate environmental impacts by using fossil fuels. Currently, fossil fuels are still available and energy production from fossil fuel is supported by transportation and distribution infrastructures, whereas hydrogen production from renewable resources and storage/transportation/distribution of hydrogen are still being investigated. Hence, onsite on-demand hydrogen generation from hydrocarbon-based fuels can be a potential solution for the seamless transition from a fossil-fuel economy to a hydrogen economy. There are many difficulties in the reforming of fossil fuel-derived feedstocks, for example, (1) it is more difficult to reform long-chain hydrocarbons, (2) aromatic compound formation during reforming will cause fouling problems [16], and (3) sulfur in fossil fuel feedstocks will deactivate most of the heterogeneous reforming catalysts [92]. Therefore, the development of noncatalytic SCWG that can generate hydrogen-rich gases is highly desirable when petroleum-based feedstocks are used.

High-temperature noncatalytic SCWGs of liquid-type feedstocks offer various advantages. (1) Desulfurization in the upstream of reforming step can be eliminated, which is important for catalyst lifetime. (2) Hydrogen-rich gas can be produced without the formation of carbon from the thermodynamic view point; this can offer

long-term operations without interrupting catalyst deactivation. (3) The use of bulky WGS reactors, which are typically needed in conventional reformers, can be eliminated because the high water content in supercritical water promotes the in situ WGS production of low CO contents. It should be noted that the volume of WGS catalyst is around six times larger than that of the reforming catalyst due to the low reaction rate of WGS reactions at low temperatures [9]. (4) The handling and storage of liquid-type feedstocks is easier than those of hydrogen, and this can eliminate bulky containers or liquefaction costs. (5) Various feedstock from oxygenated hydrocarbon or liquid fossil fuel can be effectively reformed.

Table 6.9 shows the summary of SCWG using fossil fuels and their model compounds as a feedstock. The SCWG of diesel fuel was studied in the presence of commercial SR catalysts [146]. For process simulations, *n*-decane was used as the diesel model compound. Without catalysts, only a small amount of hydrogen (~0.06 mol/mol) was produced, while with a methanation catalyst, the hydrogen gas yield was ~3.8 mol/mol *n*-decane at 550 °C 250 bar, 10 vol% *n*-decane in feed, and 10 s. This value is almost 100% of the equilibrium hydrogen gas yield. The test with diesel feed using a catalyst containing 32.4 wt% NiO and 4 wt% CaO showed that that longer residence times were required to reform diesel as compared with *n*-decane to increase the hydrogen gas yield. Hydrogen gas yield of 2.5 mol/mol diesel was achieved at 550 °C, 250 bar, 2.5 vol% diesel, and 40 s. Lee's group at Missouri University of Science and Technology investigated the reformation of civilian jet fuel (Jet-A) and military logistic aviation fuel (JP-8) for hydrogen production [91,147,148]. Both fuels are a blend of hydrocarbons and the number of carbon bonds, including straight chain, branched, and cyclic carbons, varied from 7 to 17 with an average carbon number of 12. The model compound used for simulations and calculations was *n*-dodecene. The sulfur contents were 0.099 wt% for Jet-A and 0.081 wt% for JP-8. Both the fuels were used as-received without further purification. A noncatalytic reforming study with JP-8 feed in supercritical water showed that high reaction temperatures were needed to increase the hydrogen production [148]. At 705 °C and 239 bar, which is close to the maximum allowable temperature for the reactor made of Inconel 625 grade I, the hydrogen content in the gaseous product was 37.3 mol%; further, this was accompanied by high CO (17.1 mol%) and CO_2 (8 mol%) contents. At temperatures below 600 °C, only a small amount of hydrogen was produced by direct C−H bond cleavages. Organosulfur compounds in the feed reacted with supercritical water and produced H_2S gas. A kinetic study that was performed based on the assumption that the main reactions were pyrolysis and reformation of hydrocarbons showed that the optimal reaction conditions for the SCWG of JP-8 feed was outside the permissible operating-range temperature of the Inconel 625 grade I reactor [147]. A more detailed study was conducted with Haynes® 230® alloy as a new reactor material to investigate higher temperature ranges in jet fuel reforming. This reactor material allows for operations at 800 °C at 360 bar. The

TABLE 6.9 Summary of SCWG Experiment Results and Theoretical Hydrogen Gas Yields Using Fossil Fuels and Their Model Compounds as Feedstocks

Feedstocks	Catalysts	Reactor Type (Reactor Material)	Experiment Conditions	CE (%)	Theoretical Max H_2 Yield (mol H_2/mol feedstock)	Equilibrium H_2 Yield (mol H_2/mol feedstock)	Experimental H_2 Yield (mol H_2/mol feedstock)	Refs
n-decane	Probe D (32.4 wt% NiO and 4 wt% CaO)	Flow reactor Na	250 bar; 550 °C; 10 vol%; 10 s	NA[1]	31[2]	3.7	~3.8	Pinkwart et al., 2004 [146]
Diesel	Probe D (32.4 wt % NiO and 4 wt % CaO)	Flow reactor Na	250 bar; 550 °C; 10 vol%; 40 s	NA[1]		3.7[2]	~2.5	
Jet-A	No	Continuous tubular reactor Haynes® 230®	241 bar; 765 °C; 6.5 wt%; 159 s	70	36[3]	20[3]	5.3	Picou et al., 2009 [91]
Isooctane	No	Continuous tubular reactor Haynes® 230®	250 bar; 767 °C; 6.3 wt%; 106 s	75	25	13.6	12.4	Sutanti et al., 2011 [95]

[1] *Not available.*
[2] *Calculated based on* n-*decane as a model compound.*
[3] *Calculated based on 1-dodecene as a model compound.*

hydrogen gas yield and CE increased as the residence time increased, which indicates that the residence time played an important role in the gasification behavior of the long-chain hydrocarbon. The maximum hydrogen gas yield was 5.3 mol/mol fuel at 765 °C, 241 bar, and 159 s, which was 14% of the theoretical maximum. When air was added to the system to perform autothermal reforming, a high CE of 94% was achieved. The addition of oxygen did not encourage the hydrogen gas yield with residence times of 151 s.

The noncatalytic reforming of isooctane in supercritical water, which is a model compound of gasoline, has been investigated by the Korea Institute of Science and Technology group [60,95,97]. Temperatures of 593–765 °C, residence times of 6–120 s, and various oxidant (hydrogen peroxide) amounts were explored using two kinds of reactor materials, Hastelloy C276 and Haynes® 230® alloy. The Haynes® 230® alloy is more suitable for higher temperature gasification investigations than Hastelloy C-276. Two types of reactor configurations—downdraft and updraft—were tested to enhance the hydrogen gas yield [60]. At low temperatures and short residence times, hydrogen peroxide promoted the hydrogen production yield, while at high temperatures and long residence times, the hydrogen yield decreases when hydrogen peroxide was added. In the absence of catalysts and oxidants, the best hydrogen yield was 12.4 mol/mol isooctane, and this is ~91.2% of the equilibrium value and ~50% of the theoretical maximum.

6.6 CHALLENGES/OUTLOOK

Due to the higher cost of hydrogen liquefaction and distribution than the onsite price, onboard reforming methods appear to be a promising solution for developing hydrogen-based energy systems. The combination of the unique physical properties of supercritical water and the performance of supercritical water in the reforming of liquid-type feedstocks make SCWG a promising approach for producing onsite hydrogen. However, some challenges have to be overcome for the large-scale commercialization.

1. Energy efficiency, heat transfer, and recovery issue

   As mentioned previously, one of the advantages of SCWG is that feedstocks with higher water contents (e.g. bioethanol and crude glycerol) can be effectively reformed in supercritical water without drying water. High amounts of water content in SCWG are beneficial for enhancing the hydrogen gas yield via WGS reactions (Eqn (6.3)). On the other hand, due to the endothermic nature of SCWG, high external energy is required to increase the reaction temperature to enhance the hydrogen gas yield (Eqn (6.6)). The energy required to heat water will significantly affect the overall energy efficiency of SCWG. Therefore, several points need to be addressed for higher energy efficiency as follows:

   a. The overall SCWG process needs to be combined with an efficient heat recovery unit. The heat for heating the water can be largely recovered by designing highly efficient heat exchangers. Efficient heat exchange between the feed and product is the primary goal of SCWG heat recovery systems.

   b. Rapid heating is required to avoid the tar/coke formations that can possibly occur when the feedstock has a slow heating rate under the subcritical condition [149]. Improving the heat transfer in the heating section can delay the catalyst deactivation [68]. Moreover, heat transfers in the heating section play a significant role in SCWG. The heat transfer coefficient itself varies with temperature due to the physical properties of water. The heat transfer coefficient can be obtained from the relation $Nu = 0.0135Re^{0.85}Pr^{0.8}$ [150]. Near the pseudocritical temperature, the heat transfer coefficient increases due to a drastic increase in the specific heat as the thermal conductivity decreases. Since the temperature increases above the pseudocritical temperature, the overall heat transfer coefficient decreases due to drastic decreases in the specific heat and continuous decrease in the thermal conductivity [151]. The management of heat transfer and heat loss issues will have significant effects on the overall efficiency.

   c. The overall efficiency of SCWG significantly depends on the type and concentration of feedstocks [152]. Feedstocks with high heating values increase the energy efficiency. The order of heating values of several feedstocks is as follows: high-heating-value diesel > gasoline > dimethyl ether > ethanol > methanol. The higher concentrations of feedstock also contribute positively to the energy efficiency.

2. Suitable reactor materials for high-temperature and high-pressure operations.

   Alloy-type materials, which are commonly used for high-temperature and high-pressure water operations to avoid corrosion, are quite expensive. Typically, alloy reactors are made of Ni-based materials, and the wall effects will affect the reactions, thereby leading to uncertain results [52,125]. On the other hand, the wall effect can also support the reaction without the utilization of heterogeneous catalysts. Corrosion due to the presence of salts or alkalis and even due to the

properties of supercritical water itself is often observed during reforming using Ni-based alloy materials. A more detailed study is necessary to obtain a deeper understanding of corrosion control during SCWG. The existence of corrosion-resistant materials is still to be established.

3. Deactivation of heterogeneous catalysts and recovery of homogeneous catalysts.

   Heterogeneous catalysts can be easily deactivated in the presence of sulfur-, nitrogen-, or other heteroatom-containing compounds in the feed. In order to increase the catalyst lifetime, the desulfurization unit or absorption unit on the upstream of the reforming step may be required to remove the sulfur- and nitrogen-containing compounds. Good control of the heating rate and optimization of operating variables are required to avoid carbon formation; this will also contribute to the catalyst deactivation. In some cases, homogeneous catalysts can increase the hydrogen gas yield better than heterogeneous catalysts. On the other hand, homogeneous catalysts also contribute to the corrosion problem and plugging due to low salt solubility in supercritical water. Homogeneous catalyst recovery also becomes an emerging problem since it is difficult to separate and regenerate the homogeneous type.

4. High-temperature operations associated with noncatalytic gasification must be optimized.

   Because of the deactivation of heterogeneous catalysts and the difficulties with homogeneous catalysts, noncatalytic SCWG is a highly promising approach. The optimization of operating conditions such as temperature, pressure, concentration, and residence time and reactor designs for different feedstocks are necessary to achieve high efficiencies.

5. Cost of liquid-type feedstocks from renewable sources.

   In 2002, the IEA estimated the production cost of fuel; the estimations of the production costs of gasoline from petroleum ($0.22/l gasoline equivalent) and ethanol from poplar ($0.27/l gasoline equivalent) are comparable [153]. The ethanol cost from cane remained low and will be on parity with gasoline before 2015–2020. The current cost analyses from the same organization reported that the retail price (untaxed) of ethanol from cellulosic biomass will be on parity with petroleum gasoline around 2030 for low-cost scenarios and around 2050 for high-cost scenarios [154]. The low-cost scenario anticipates minimal impacts of rising oil prices on the biofuel production cost, while the high-cost scenario considers the greater impacts of oil prices on the biofuel production. It is to be noted that the price should include the separation price for obtaining pure ethanol due to the azeotropic characteristics of the ethanol–water mixture. The low ethanol concentrations from fermentation can be reformed directly in supercritical water excluding the drying cost. Crude glycerol from biodiesel plants is a potential feedstock for hydrogen production in supercritical water because it is cheap and abundant and separation processes may not be necessary. Hence, more SCWG studies are necessary for developing efficient hydrogen production from crude glycerol.

6.7 CONCLUSION

Hydrogen is considered to be one of the most promising clean energy sources of the future and can be used in mobile and stationary applications. Extensive investigations have been conducted on SCWG in recent years to develop efficient hydrogen production technologies. Due to the unique physical properties of supercritical water, SCWG offers many benefits for reforming various types of hydrocarbons for hydrogen production. Feedstock flexibility, faster reaction, homogeneous phases of feedstocks, reaction intermediates and produced gases, short residence time, compactness of reactor and subsequent units, high conversions, and low carbon monoxide contents are the advantages of SCWG. Although continuous flow processing of liquid-type feedstocks has demonstrated that high conversion to hydrogen can be obtained, several challenges need to be overcome for commercialization. With further development of liquid-type feedstock reforming in supercritical water, SCWG will play a significant role in the development of sustainable energy systems.

Acknowledgments

The authors acknowledge Korea Research Council of Fundamental Science and Technology (KRCF) and Korea Institute of Science and Technology (KIST) for "National Agenda Program (NAP)" for support.

References

[1] Agency IE. Energy technology analysis: prospects for hydrogen and fuel cells. Paris: OECD/IEA; 2005.
[2] Navarro RM, Sanchez-Sanchez MC, Alvarez-Galvan MC, Valle FD, Fierro JLG. Energy Environ Sci 2009;2:35–54.
[3] Saxena RC, Seal D, Kumar S, Goyal HB. Renew Sustain Energy Rev 2008;12:1909–27.
[4] Ewan BCR, Allen RWK. Int J Hydrogen Energy 2005;30:809–19.
[5] Wells SA, Sartbaeva A, Kuznetsov VL, Edwards PP. Hydrogen economy. In: Crabtree RH, editor. Energy production and storage: inorganic chemical strategies for a warming world. CT: John Wiley & Sons; 2010. p. 309–40.
[6] Holladay JD, Hu J, King DL, Wang Y. Catal Today 2009;139:244–60.
[7] Goltsov VA, Veziroglu TN, Goltsova LF. Int J Hydrogen Energy 2006;31:153–9.

[8] Kirtay E. Energy Convers Manag 2011;52:1778–89.
[9] Qi A, Peppley B, Karan K. Fuel Process Technol 2007;88:3–22.
[10] Rutz D, Janssen R. Bio fuel technology handbook. Munchen, Germany: WIP Renewable Energies; 2007.
[11] IEA Energy Technology Essentials. Hydrogen production and distribution. OECD/IEA; 2007.
[12] C.F.C. Partnership. Department of Energy Targets, http://www.fuelcellpartnership.org/~cafcp12/progress/technology/doetargets.
[13] Lemus RG, Martiez Duart JM. Int J Hydrogen Energy 2010;35:3929–36.
[14] Ohmori T. EOS-SCx; 2004.
[15] Wagner W, Pruss A. J Phys Chem Ref Data 2002;31:387–535.
[16] Guo Y, Wang SZ, Xu DH, Gong YM, Ma HH, Tang XY. Renew Sustain Energy Rev 2010;14:334–43.
[17] Kuhlmann B, Arnett EM, Siskin M. J Org Chem 1994;59:3098–101.
[18] Aida TM, Ikarashi A, Saito Y, Watanabe M, Smith Jr RL, Arai K. J Supercrit Fluids 2009;50:257–64.
[19] Chandler K, Deng F, Dillow AK, Liotta CL, Eckert CA. Ind Eng Chem Res 1997;36:5175–9.
[20] Ikushima Y, Hatakeda K, Sato O, Yokoyama T, Arai M. J Am Chem Soc 2000;122:1908–18.
[21] Glaser R, Brown JS, Nolen SA, Liotta CL, Eckert CA. Abstr Papers Am Chem Soc 1999;217:U820.
[22] Nolen SA, Liotta CL, Eckert CA, Glaser R. Green Chem 2003;5:663–9.
[23] Tsujino Y, Wakai C, Matubayashi N, Nakahara M. Chem Lett 1999;28:287–8.
[24] Kruse A, Dinjus E. J Supercrit Fluids 2007;39:362–80.
[25] Weingartner H, Franck EU. Angew Chem Int Ed 2005;44:2672–92.
[26] Marrone PA, Hong GT. J Supercrit Fluids 2009;51:83–103.
[27] Hua I, Hoechemer RH, Hoffmann MR. J Phys Chem 1995;99:2335–42.
[28] Zahn D. Eur J Org Chem 2004;2004:4020–3.
[29] Townsend SH, Abraham MA, Huppert GL, Klein MT, Paspek SC. Ind Eng Chem Res 1988;27:143–9.
[30] Tsao CC, Zhou Y, Liu X, Houser TJ. J Supercrit Fluids 1992;5:107–13.
[31] Bühler W, Dinjus E, Ederer HJ, Kruse A, Mas C. J. Supercrit Fluids 2002;22:37–53.
[32] Wang S, Guo Y, Wang L, Wang Y, Xu D, Ma H. Fuel Process Technol 2011;92:291–7.
[33] Landau LD, Lifshitz EM. Fluid mechanics. Oxford: Pergamon Press; 1987.
[34] Olesik SV, Woodruff JL. Anal Chem 1991;63:670–6.
[35] Fernandez DP, Goodwin ARH, Lemmon EW, Sengers JMHL, Williams RC. J Phys Chem Ref Data 1997;26:1125–66.
[36] Solubility of Gases in Water, http://www.engineeringtoolbox.com/gases-solubility-water-d_1148.html.
[37] Valyashko VM. Pure Appl Chem 1997;69:2271–80.
[38] Tom JW, Debenedetti PG. J Aerosol Sci 1991;22:555–84.
[39] Hakuta Y, Hayashi H, Arai K. Curr Opin Solid State Mater Sci 2003;7:341–51.
[40] Viswanathan R, Lilly GD, Gale WF, Gupta RB. Ind Eng Chem Res 2003;42:5535–40.
[41] Lummen N, Kvamme B. Phys Chem Chem Phys 2008;10:6405–16.
[42] Adschiri T, Kanazawa K, Arai K. J Am Ceram Soc 1992;75:1019–22.
[43] Akiya N, Savage PE. Chem Rev 2002;102:2725–50.
[44] Partay L, Jedlovszky P. J Chem Phys 2005;123:024502–5.
[45] Nakahara M, Matubayasi N, Wakai C, Tsujino Y. J Mol Liq 2001;90:75–83.
[46] Hoffmann MM, Conradi MS. J Am Chem Soc 1997;119:3811–7.
[47] Beta IA, Li JC, Bellissent-Funel MC. Chem Phys 2003;292:229–34.
[48] Svishchev IM, Plugatyr AY. J Phys Chem B 2005;109:4123–8.
[49] Moriya T, Enomoto H. Polym Degrad Stab 1999;65:373–86.
[50] Houser TJ, Tsao C-C, Dyla JE, Van Atten MK, McCarville ME. Fuel 1989;68:323–7.
[51] Li L, Portela JR, Vallejo D, Gloyna EF. Ind Eng Chem Res 1999;38:2599–606.
[52] Yu D, Aihara M, Antal MJ. Energy Fuels 1993;7:574–7.
[53] Park KC, Tomiyasu H. Chem Commun 2003:694–5.
[54] Sato T, Kurosawa S, Smith RL, Adschiri T, Arai K. J Supercrit Fluids 2004;29:113–9.
[55] Andrea K. Biofuels, Bioprod Biorefin 2008;2:415–37.
[56] Lu YJ, Guo LJ, Ji CM, Zhang XM, Hao XH, Yan QH. Int J Hydrogen Energy 2006;31:822–31.
[57] Peterson AA, Vogel F, Lachance RP, Froling M, Antal JMJ, Tester JW. Energy Environ Sci 2008;1:32–65.
[58] Matsumura Y. Energy Convers Manag 2002;43:1301–10.
[59] Taylor JD, Herdman CM, Wu BC, Wally K, Rice SF. Int J Hydrogen Energy 2003;28:1171–8.
[60] Susanti RF, Veriansyah B, Kim J-D, Kim J, Lee Y-W. Int J Hydrogen Energy 2010;35:1957–70.
[61] Calzavara Y, Joussot-Dubien C, Boissonnet G, Sarrade S. Energy Convers Manag 2005;46:615–31.
[62] Watanabe M, Sato T, Inomata H, Smith RL, Arai K, Kruse A, et al. Chem Rev 2004;104:5803–22.
[63] Elliott DC, Sealock LJ. Ind Eng Chem Prod Res Devel 1983;22:426–31.
[64] Minowa T, Inoue S. Renewable Energy 1999;16:1114–7.
[65] Minowa T, Ogi T. Catal Today 1998;45:411–6.
[66] Minowa T, Zhen F, Ogi T. J Supercrit Fluids 1998;13:253–9.
[67] Elliott DC. Biofuels, Bioprod Biorefin 2008;2:254–65.
[68] Xu X, Matsumura Y, Stenberg J, Antal MJ. Ind Eng Chem Res 1996;35:2522–30.
[69] Antal MJ, Allen SG, Schulman D, Xu X, Divilio RJ. Ind Eng Chem Res 2000;39:4040–53.
[70] Michael Jerry Antal J, Xu X. U. S. DOE hydrogen program annual review. Alexandria: Virginia; 1998.
[71] Kruse A, Dinjus E. Angew Chem Int Ed 2003;42:909–11.
[72] Elliott DC, Sealock LJ, Baker EG. Ind Eng Chem Res 1993;32:1542–8.
[73] Sato T, Osada M, Watanabe M, Shirai M, Arai K. Ind Eng Chem Res 2003;42:4277–82.
[74] Waldner MH, Vogel F. Ind Eng Chem Res 2005;44:4543–51.
[75] Yoshida T, Oshima Y, Matsumura Y. Biomass Bioeng 2004;26:71–8.
[76] Osada M, Hiyoshi N, Sato O, Arai K, Shirai M. Energy Fuels 2007;21:1400–5.
[77] Osada M, Hiyoshi N, Sato O, Arai K, Shirai M. Energy Fuels 2008;22:845–9.
[78] Osada M, Hiyoshi N, Sato O, Arai K, Shirai M. Energy Fuels 2007;21:1854–8.
[79] Elliott DC, Neuenschwander GG, Hart TR, Butner RS, Zacher AH, Engelhard MH, et al. Ind Eng Chem Res 2004;43:1999–2004.
[80] Elliott DC, Hart TR, Neuenschwander GG. Ind Eng Chem Res 2006;45:3776–81.
[81] Elliot DC, Sealock JL. Nickel/ruthenium catalyst and method for aqueous phase reactions. U.S. Patent 5,814,112; 1998.
[82] Peterson AA, Vontobel P, Vogel F, Tester JW. J Supercrit Fluids 2008;43:490–9.
[83] Kruse A, Meier D, Rimbrecht P, Schacht M. Ind Eng Chem Res 2000;39:4842–8.
[84] Yanik J, Ebale S, Kruse A, Saglam M, Yüksel M. Int J Hydrogen Energy 2008;33:4520–6.
[85] Thompson JC, He BB. Appl Eng Agricul 2006;22:261–5.

[86] Schmieder H, Abeln J, Boukis N, Dinjus E, Kruse A, Kluth M, et al. J Supercrit Fluids 2000;17:145–53.
[87] Byrd AJ, Pant KK, Gupta RB. Fuel 2008;87:2956–60.
[88] Matsumura Y, Minowa T, Potic B, Kersten SRA, Prins W, van Swaaij WPM, et al. Biomass Bioeng 2005;29:269–92.
[89] Basu P, Mettanant V. Int J Chem React Eng 2009;7:1–61.
[90] Kruse A. J Supercrit Fluids 2009;47:391–9.
[91] Picou JW, Wenzel JE, Lanterman HB, Lee S. Energy Fuels 2009;23:6089–94.
[92] Gadhe JB, Gupta RB. Int J Hydrogen Energy 2007;32:2374–81.
[93] Boukis N, Diem V, Habicht W, Dinjus E. Ind Eng Chem Res 2003;42:728–35.
[94] Guo LJ, Lu YJ, Zhang XM, Ji CM, Guan Y, Pei AX. Catal Today 2007;129:275–86.
[95] Susanti RF, Nugroho A, Lee J, Kim Y, Kim J. Int J Hydrogen Energy 2011;36:3895–906.
[96] Resende FLP, Fraley SA, Berger MJ, Savage PE. Energy Fuels 2008;22:1328–34.
[97] Veriansyah B, Kim J, Kim JD, Lee YW. Int J Green Energy 2008;5:322–33.
[98] Bond GC, Webb G, Ross JRH. Metal catalysed methanation and steam reforming. In: Bond GC, Webb G, editors. Catalysis. London: The Royal Society of Chemistry; 1985. p. 1–45.
[99] Rostrup-Nielsen JR. J Catal 1973;31:173–99.
[100] Penninger JML, Rep M. Int J Hydrogen Energy 2006;31:1597–606.
[101] Byrd AJ, Pant KK, Gupta RB. Energy Fuels 2007;21:3541–7.
[102] Fischer F, Tropsch H, Dilthey P. Brennst Chem 1925;6:265.
[103] Seglin L, Geosits R, Franko BR, Gruber G. Survey of methanation chemistry and processes. In: Seglin L, editor. Methanation of synthesis gas. Washington, DC: American Chemical Society; 1975. p. 1–30.
[104] Jin H, Lu Y, Guo L, Cao C, Zhang X. Int J Hydrogen Energy 2010;35:3001–10.
[105] Lee S. Alternative fuels. Washingthon, DC: Taylor and Francis; 1996.
[106] Chakinala A, Brilman D, Swaaij W, Kersten S. Ind Eng Chem Res 2010;49:1113–22.
[107] Gadhe JB, Gupta RB. Ind Eng Chem Res 2005;44:4577–85.
[108] Byrd AJ, Pant KK, Gupta RB. Ind Eng Chem Res 2007;46:3574–9.
[109] Palo DR, Dagle RA, Holladay JD. Chem Rev 2007;107:3992–4021.
[110] Boukis N, Diem V, Galla U, Dinjus E. Combust Sci Technol 2006;178:467–85.
[111] Haryanto A, Fernando S, Murali N, Adhikari S. Energy Fuels 2005;19:2098–106.
[112] Ni M, Leung DYC, Leung MKH. Int J Hydrogen Energy 2007;32:3238–47.
[113] Luterbacher JS, Frölling M, Vogel F, Maréchal F, Tester JW. Environ Sci Technol 2009;43:1578–83.
[114] ScienceDaily. New reactor puts hydrogen from renewable fuels within reach. http://www.sciencedaily.com/about.htm.
[115] Patzek TW. Sustainability of the corn-ethanol biofuel cycle. Berkeley, CA: College of Engineering; 2004.
[116] Rabe S, Nachtegaal M, Ulrich T, Vogel F. Angew Chem Int Ed 2010;49:6434–7.
[117] Arita T, Nakahara K, Nagami K, Kajimoto O. Tetrahedron Lett 2003;44:1083–6.
[118] Therdthianwong S, Srisiriwat N, Therdthianwong A, Croiset E. J Supercrit Fluids 57: 58–65.
[119] Vaidya PD, Rodrigues AE. Ind Eng Chem Res 2006;45:6614–8.
[120] Schanzenbacher J, Taylor JD, Tester JW. J Supercrit Fluids 2002;22:139–47.
[121] Mok WSL, Antal MJ. Ind Eng Chem Res 1992;31:1157–61.
[122] Amin S, Reid RC, Modell M. Intersociety conference on environmental systems. San Francisco; 1975. ASME Paper 75-ENAS-21.
[123] Hao XH, Guo LJ, Mao X, Zhang XM, Chen XJ. Int J Hydrogen Energy 2003;28:55–64.
[124] Lee I-G, Kim M-S, Ihm S-K. Ind Eng Chem Res 2002;41:1182–8.
[125] Lee I-G, Ihm S-K. Ind Eng Chem Res 2009;48:1435–42.
[126] Watanabe M, Inomata H, Arai K. Biomass Bioeng 2002;22:405–10.
[127] Watanabe M, Inomata H, Osada M, Sato T, Adschiri T, Arai K. Fuel 2003;82:545–52.
[128] Sinag A, Kruse A, Rathert J. Ind Eng Chem Res 2004;43:502–8.
[129] Sinag A, Kruse A, Schwarzkopf V. Ind Eng Chem Res 2003;42:3516–21.
[130] Goodwin AK, Rorrer GL. Ind Eng Chem Res 2008;47:4106–14.
[131] Susanti RF, Dianningrum LW, Yum T, Kim Y, Lee BG, Kim J. Int J Hydrogen Energy 2012;37:11677–90.
[132] Williams PT, Onwudili J. Ind Eng Chem Res 2005;44:8739–49.
[133] Minowa T, Fang Z, Ogi T, Varhegyi G. J Chem Eng Jpn 1998;31:131–4.
[134] Minowa T, Ogi T, Yokoyama S-y. Chem Lett 1995;24:937–8.
[135] Minowa T, Fang Z. J Chem Eng Jpn 1998;31:488–91.
[136] Minowa T, Zhen F, Ogi T, Varhegyi G. J Chem Eng Jpn 1997;30:186–90.
[137] Holgate HR, Meyer JC, Tester JW. AIChE J 1995;41:637–48.
[138] Kabyemela BM, Adschiri T, Malaluan RM, Arai K. Ind Eng Chem Res 1999;38:2888–95.
[139] Sims R, Taylor M, Saddler J, Mabee W. From 1st to 2nd generation biofuel technologies. International Energy Agency; 2008.
[140] Pagliaro M, Rossi M. The future of glycerol. 2nd ed. Cambridge: The Royal Society of Chemistry; 2010.
[141] Onwudili JA, Williams PT. Fuel 2010;89:501–9.
[142] Kersten SRA, Potic B, Prins W, Van Swaaij WPM. Ind Eng Chem Res 2006;45:4169–77.
[143] Xu D, Wang S, Hu X, Chen C, Zhang Q, Gong Y. Int J Hydrogen Energy 2009;34:5357–64.
[144] May A, Salvad J, Torras C, Montan D. Chem Eng J 2010;160:751–9.
[145] Hungate RE. Cell Mol Life Sci 1982;38:189–92.
[146] Pinkwart K, Bayha T, Lutter W, Krausa M. J Power Sources 2004;136:211–4.
[147] Lee S, Lanterman HB, Picou J, Wenzel JE. Energy Sources, Part A 2009;31:1813–21.
[148] Lee S, Lanterman HB, Wenzel JE, Picou J. Energy Sources, Part A 2009;31:1750–8.
[149] Kruse A, Henningsen T, Sinag A, Pfeiffer J. Ind Eng Chem Res 2003;42:3711–7.
[150] Yamagata K, Nishikawa K, Hasegawa S, Fujii T, Yoshida S. Int J Heat Mass Transfer 1972;15:2575–93.
[151] Basu P. Biomass gasification and pyrolysis: practical design and theory. Oxford: Elsevier; 2010.
[152] Nakamura A, Kiyonaga E, Yamamura Y, Shimizu Y, Minowa T, Noda Y, et al. J Chem Eng Jpn 2008;41:817–28.
[153] An international perspective: biofuels for transport. International Energy Agency; 2004.
[154] Technology roadmap: biofuels for transport. Paris: International Energy Agency; 2011.
[155] Bandura AV, Lvov SN. J Phys Chem Ref Data 2006;35:15–30.
[156] Lu Y, Guo L, Zhang X, Yan Q. Chem Eng J 2007;131:233–44.
[157] Sinag A, Kruse A, Rathert J. Ind Eng Chem Res 2004;43:502–8.

CHEMISTRY

SUPERCRITICAL FLUID TECHNOLOGY

FOR ENERGY AND ENVIRONMENTAL APPLICATIONS

Edited by
VLADIMIR ANIKEEV
MAOHONG FAN

Supercritical Fluid Technology for Energy and Environmental Applications explores in-depth the fundamental principles involved in the preparation and characterization of supercritical fluids used in the energy production and other environmental applications. By focusing on the critical issues scientists and engineers are faced with in applications of Supercritical Fluids, this book then explores the innovative solutions and current challenges which need to be overcome in the future during the applications of Supercritical Fluid technology. Because Supercritical Fluid technology has many unique applications through various industries and academic fields, this book has a wide range of uses across many different professions and experience levels. *Supercritical Fluid Technology for Energy and Environmental Applications* is a must-have for physical chemists, chemical engineers, and anyone who researches new technologies in academia, government, and corporate environments.

Supercritical Fluid Technology for Energy and Environmental Applications

- Reviews the theory and thermodynamic properties of supercritical fluids
- Relates theory and properties of the particular supercritical fluid to its various applications
- Includes the most recent applications of supercritical fluids, including energy generation, catalysis and environmental protection

ELSEVIER
store.elsevier.com

ISBN 978-0-444-62696-7